Probes) to detect nuclei. Finally, the cells were washed three times with PBS, immersed in PermaFluor aqueous mounting reagent (Immunon, Pittsburgh, PA, USA), and observed under a MRC-1024 confocal laser microscope (Bio-Rad, Richmond, CA, USA).

2.8. NF-κB reporter luciferase assay

HEK293^{Cont} or HEK293^{poNOD2} cells (8×10^4/well in a 24-well plate) were transfected for 4 h using Lipofectamine™ reagent with 0.2 μg of pGLM-ENH-luci vector (Shimosato et al., 2006; Ueda et al., 1997), which encodes human NF-κB gene A1 and A2 sites. After a 24-h stimulation with various concentrations of muramyl dipeptide (MDP; Invivogen, San diego, CA, USA), luciferases were measured according to the manufacturer's protocol (Promega, Tokyo, Japan). In some experiments, cytochalasin D (1 μM) was added directly to the cell culture medium for 30 min to allow better stimulation by MDP (Magalhaes et al., 2005). The relative index (RI) was estimated from the resonance units (RU) using the following equation: RI = [(RU in stimulated cultures) − (RU in background)]/[(RU in non-stimulation) − (RU in background)]. All assays were conducted at least three times in triplicates.

2.9. Real-time quantitative PCR

Total RNA was isolated from various adult and newborn swine tissues as described (Shimosato et al., 2005b; Tohno et al., 2006). Briefly, cDNAs were prepared by reverse transcription of 1 μg total RNA using QuantiTect Reverse Transcription Kit (Qiagen). An equivalent volume of cDNA solution from each sample was used for quantification of poNOD2-specific cDNA by real-time quantitative PCR. The reactions occurred on a 7300 real-time PCR System (Applied Biosystems, Warrington, UK) using Platinum SYBR Green qPCR SuperMix UDG with ROX (Invitrogen) with primers listed in Table 1. The reaction was initiated by denaturation for 2 min at 95 °C, followed by 40 cycles of 15 s at 95 °C, 30 s at 60 °C, and 30 s at 72 °C. The results are expressed as the relative mRNA index, calculated as the index (NOD2 mRNA copy number/β-actin mRNA copy number) for the test sample divided by the index in esophagus. In the control tubes, poly $(A)^+$ RNA samples were used as templates to examine the presence of contaminating genomic DNA. Amplification products of contaminants such as primer dimers were not detected by SYBR green chemistry using serial dilutions of cDNA. DNA sequencing confirmed that the amplified cDNAs were identical to the bases 1033–1098 of poNOD2.

2.10. Measurement of NOD2 expression

Single-cell suspensions from ileal Pps and MLNs were prepared by cutting the specimens into small fragments gently pressing through a nylon mesh and washing 3× in complete RPMI 1640 medium (Sigma) supplemented with 10% FCS (Hyclone Co., Logan, USA) (Tohno et al., 2006). Residual erythrocytes were lysed by resuspension of the cells in hypotonic salt solution (0.2% NaCl), followed by hypertonic rescue in an equal volume of 1.5% NaCl. After washing 3× with a staining buffer (PBS containing 2% FCS and 0.1% sodium azide), the cells were treated with 2 mg/mL collagenase (Wako, Osaka, Japan) and 0.1 mg/mL dispase (Sigma) for 30 min at 25 °C, after which the cells were passed through cell strainers (BD bioscience, Tokyo, Japan) to remove debris and connective tissue. Total RNA was isolated from 2×10^6 ileal Pps and MLNs cells treated with MDP (1, 10, 50 μg/mL), CpG2006-TGTT (0.1, 1, 5 μM; Operon, Tokyo, Japan; Shimosato et al., 2006), Pam3Cys (0.1, 1, 10 ng/mL; EMC Microcollection, Tuebingen, Germany), *Lactobacillus* (*L.*) *gasseri* JCM1131^T (1, 10, 100 μg/mL), or *Lactobacillus bulgaricus* NIAI B6 (1, 10, 100 μg/mL) for the indicated times at 37 °C in 5% CO_2. Three replicates were prepared for each condition. The cDNA preparation and real-time PCR were then conducted.

2.11. Statistics

All results represent the average of three to five separate experiments. The statistical significance of differences was assessed using Student's *t*-test.

3. Results and discussion

3.1. Cloning and characterization of poNOD2

The cDNA encoding poNOD2 was derived from mRNA isolated from adult swine ileal Pps. The 3′- and 5′-terminal regions of the cDNA were obtained by 3′- and 5′-RACE. The sequences were confirmed in three ileal Pps from different swine. poNOD2 cDNA contains 4460-bp, including its structural gene. The predicted open reading frame (ORF) locates between nucleotides 739 and 3777 and encodes a putative 1013-aa protein as shown in Fig. 1A. The nucleotide sequence of poNOD2 has been submitted to the DDBJ, EMBL and GenBank nucleotide databases under accession No. AB195466.

Analysis of the primary structure of poNOD2 using the SMART architecture research program identified multiple C-terminal LRR domains, a central NACHT domain and an N-terminal effector domain that contains two CARD domains (Fig. 1B). In the C-terminal region, porcine and human NOD2 have seven LRR domains, whereas mouse NOD2 has eight (Fig. 1B). Similar to human and mouse NOD2 (Inohara and Nunez, 2003), poNOD2 contains no signal peptide allowing for release of the mature proteins from intracellular compartment, suggesting that poNOD2 might be expressed mainly in the cytosol.

Comparison of the ORF nucleic acid sequences of poNOD2 with those of human and mouse NOD2 indicated 84.4 and 77.9% identity, respectively. At the deduced aa level, the corresponding identity was 81.6 and 76.6%, respectively. These results indicate that poNOD2 is more similar to human than to mouse NOD2 at both the cDNA and aa levels. In the phylogenetic analysis, poNOD2 belonged to the group containing american bison, bovine and zebu NOD2 (Fig. 2). As well as the identity, poNOD2 was more closely related to human NOD2 than mouse NOD2, supporting the notion that swine may be a model closer to human

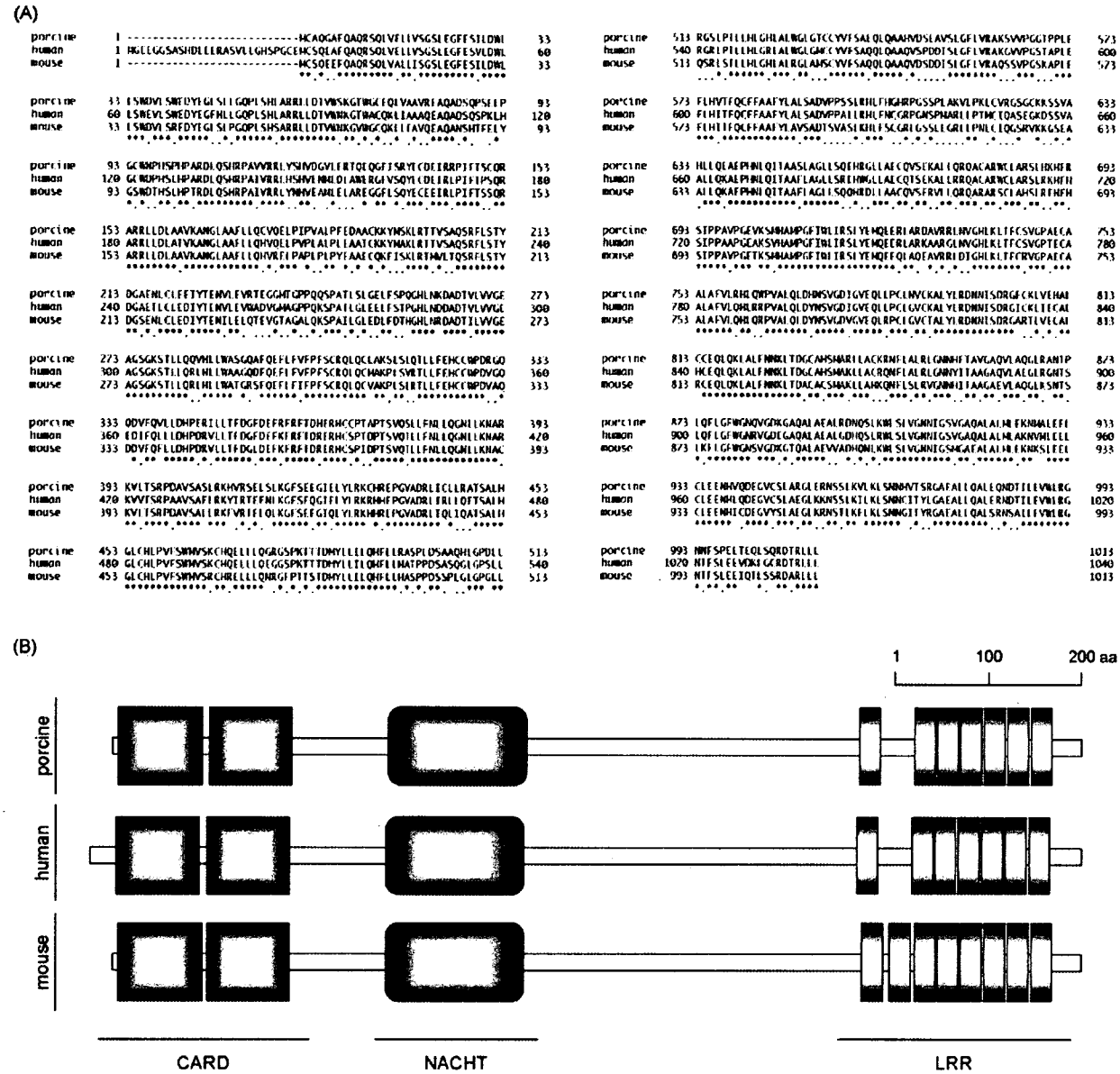

Fig. 1. Alignment and architecture of deduced aa sequences for NOD2. (A) Alignment of aa sequences of porcine, human and mouse NOD2. The numbers indicate the aa position. Identical aa residues are marked with asterisks. Similar aa residues are marked with dots. Gaps were introduced to optimize alignment. (B) Architectures of porcine, human and mouse NOD2. The protein sequences of porcine, human and mouse NOD2 were analyzed by a SMART architecture research computer program. CARD, caspase-recruitment domain; NACHT domain, domain present in NAIP, CIITA, HET-E, TP-1; LRR, leucine-rich repeats. The nucleotide sequence of poNOD2 has been submitted to the DDBJ, EMBL, and GenBank nucleotide databases under accession number AB195466.

intestinal immune system as compared with mouse (Shimosato et al., 2005b; Tohno et al., 2005b, 2006). Because swine organs are also histologically closer to human's, it should be reasonable to test swine immunological responses as human models.

3.2. Cellular localization and functional analysis of poNOD2

To elucidate the subcellular expression of poNOD2 and the signal transduction through poNOD2, we constructed poNOD2-expressing HEK293^{poNOD2} cells. RT-PCR confirmed that the mRNA for poNOD2 was expressed only in HEK293^{poNOD2} cells (Fig. 3A). Intracellular staining of HEK293^{poNOD2} cells with an anti-FLAG monoclonal Ab showed that HEK293^{poNOD2} cells were FLAG-poNOD2-positive as detected by flow cytometry (Fig. 3B). Extracellular staining showed that FLAG-poNOD2 was not detected (Fig. 3B). Similar staining patterns were observed when stained with an anti-poNOD2 polyclonal Ab (data not shown). The results were confirmed by confocal laser microscopy, showing that poNOD2 was not on cell surface (Fig. 3C-b), but was in the intracellular compartment (Fig. 3C-c) and located closely to the plasma membrane (Fig. 3C-c, arrows). No intracellular fluorescence of poNOD2 was observed in HEK293^{Cont} cells (Fig. 3C-a). Because cell surface staining

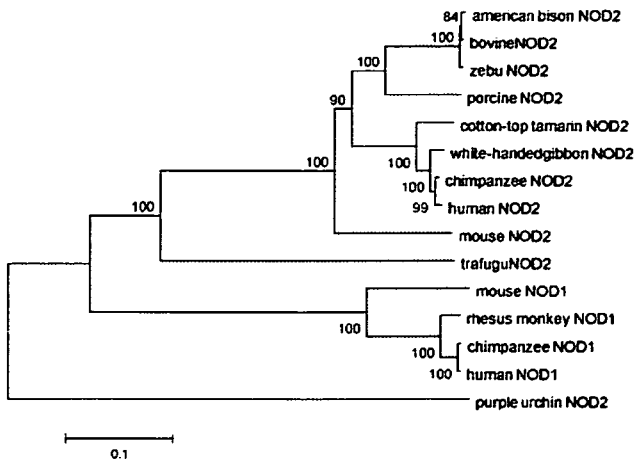

Fig. 2. A phylogenetic tree of amino acid sequences of NOD1 and NOD2. The unrooted tree was built using the neighbor-joining method based on the alignment of NOD1 and NOD2 amino acid sequences. Numbers indicate the bootstrap percentage (1000 replicates). The scale indicates the divergence time.

showed no fluorescence of poNOD2, the observed membrane-associated poNOD2 was likely on the intracellular side of the cell membrane. Furthermore, intracellular immunostaining of non-tagged poNOD2-expressing cells with an anti-poNOD2 Ab revealed that poNOD2 was located in the cytosol and also appeared enriched close to the cell membrane (Fig. 3D), indicating that the nature of the FLAG tag did not affect cellular localization. Recent evidence showed that human NOD2 in intestinal epithelial cells contains domains that associate with cell membrane, therefore it is localized not only in the cytoplasm but also at the intracellular side of the membrane (Barnich et al., 2005). Human NOD2 membrane association was reported to be required for NF-κB activation after the interaction with bacterial MDP (Barnich et al., 2005). Thus, our results suggest the similarity in subcellular localization between poNOD2 and human NOD2.

To confirm the function of poNOD2, we used MDP, a potent ligand for human and mouse NOD2 (Inohara and Nunez, 2003; Girardin et al., 2003) to examined the activation of NF-κB in HEK293^{poNOD2} cells. When stimulated by MDP, there was a significant increase in NF-κB dependent luciferase activity in HEK293^{poNOD2} cells (Fig. 3E). When HEK293^{poNOD2} cells were stimulated with 0.5 and 1 μg/mL MDP in the presence of cytochalasin D, an agent reported to increase the potency of low concentrations of MDP (Magalhaes et al., 2005; Uehara et al., 2006), there was a further enhanced activation of NF-κB in HEK293^{poNOD2} cells as compared with stimulation in the absence of cytochalasin D (Fig. 3E). In contrast, NF-κB was not activated by MDP in control HEK293^{Cont} cells (Fig. 3E). Similar activation of NF-κB was observed in the non-tagged poNOD2-expressing transfectants (data not shown). These findings suggest that poNOD2 recognizes MDP, resulting in the activation of NF-κB. However, how the bacterial MDP enters the cytoplasm is unclear. It has been reported that apical peptide transporter PEPT1 may deliver MDP and subsequently activate NF-κB in human colonic epithelial cell lines (Vavricka et al., 2004). In HEK293 cells, certain level of PEPT1 is detected and it may participate in the incorporation of dipeptides thus delivering MDP across the cell membrane (Uchiyama et al., 2003). Our results show that the cloned poNOD2 is functionally expressed in the cytoplasmic regions and has the ability to induce NF-κB activation after stimulation by MDP.

3.3. The expression of NOD2 in newborn and adult swine tissues

Although the expression of NOD2 has been analyzed in a variety of human and mouse cell lines in vitro (Sugawara et al., 2006; Gutierrez et al., 2002; Inohara and Nunez, 2003), no quantitative comparison of its tissue-specific expression has been made. It has been demonstrated that NOD2 plays a crucial role in the pathogenesis of gastrointestinal diseases such as Crohn's disease in gut (Inohara and Nunez, 2003; Girardin et al., 2003). However little is known about the expression pattern and the role of NOD2 in the newborn and adult gut. Therefore, we used real-time quantitative PCR to analyze the expression of NOD2 mRNA in newborn and adult swine tissues. As shown in Fig. 4, NOD2 mRNA was expressed at detectable levels in all newborn and adult swine tissues examined. In the newborn swine, the expression level of NOD2 mRNA varies in different organs with highest expression in the spleen and MLNs, while lower levels in colon and esophagus (Fig. 4A). It has been shown that NOD2 is mainly expressed in antigen presenting cells (APC) and epithelial cells (Strober et al., 2006). Because spleen and MLNs contain a large number of APC such as dendritic cells and macrophages (Shimosato et al., 2005b; Piguet et al., 1981), it is not surprising that higher levels of NOD2 are detected in these tissues of the newborn swine. In the newborn swine, relatively lower expression level of NOD2 was found in intestinal tissues that are directly exposed to the intestinal bacteria in the adult period. It has been reported that the expression level of NOD2 in intestinal epithelial cells is upregulated by pro-inflammatory cytokines stimulated by bacterial products (Rosenstiel et al., 2003). Therefore, our results suggest that the lower levels of NOD2 expression in immature intestinal tissues of newborn swine may be due to their insufficient exposure to intestinal bacterial flora.

On the other hand, in the adult swine, the expression levels in the intestinal tissues were relatively equal to those in MLNs and spleen, and the highest level of expression was observed in ileal Pps (Fig. 4B). Compared with newborns immediately after birth, adult intestinal tissues are continually exposed to intestinal microbial antigens. Adult intestinal tissues also directly and frequently encounter microbial antigens across the intestinal epithelial cells, in contrast to MLNs and spleen, which obtain antigens from afferent lymphatics or blood. Therefore, the different expression patterns of NOD2 in newborn and adult intestinal tissues provide the idea that the intestinal microflora directly promotes the expression of NOD2 in the intestinal tissues during postnatal development, resulting in same or higher expression levels of NOD2 in adult intestinal tissues compared with lymphoid organs, such as MLNs and spleen.

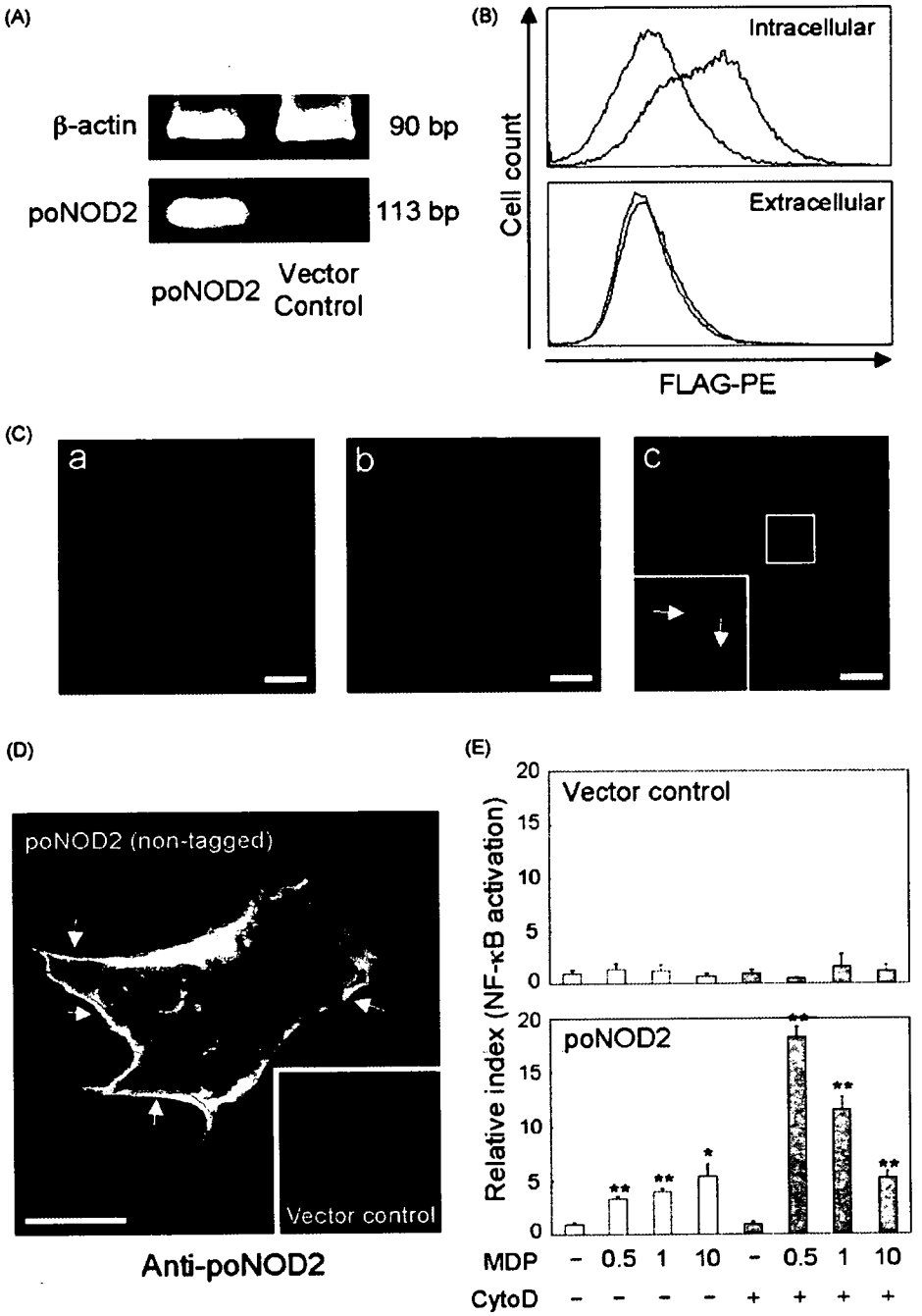

Fig. 3. The expression and function of poNOD2 in HEK293 cells. (A) The expression of poNOD2 mRNA in HEK293^{poNOD2} cells was analyzed by RT-PCR. The PCR products were detected on agarose gels. (B) The expression of poNOD2 protein in HEK293^{poNOD2} cells was detected by intracellular or extracellular staining with PE-conjugated anti-FLAG monoclonal Ab followed by flow cytometry. Blue and black lines indicate HEK293^{poNOD2} and vector control cells, respectively. (C) Cellular localization of poNOD2 was observed by confocal laser microscopy. HEK293^{Cont} (a, intracellular staining) or HEK293^{poNOD2} (b, cell surface staining; c, intracellular staining) cells were stained with anti-FLAG monoclonal Ab, followed by Alexa 647-conjugated anti-mouse IgG (blue). Inset in the panel (c) shows enlarged box areas in the box. The nuclei were stained with SYTOX orange (red). Representative sections from one of six independent experiments are shown. Scale bars = 50 μm. (D) The non-tagged poNOD2 was stained by anti-poNOD2 Ab, followed by Alexa 488-conjugated anti-rabbit IgG (green). Inset shows the cells transiently transfected with control plasmid vector. The nuclei were stained with SYTOX orange (red). Representative sections from one of six independent experiments are shown. Scale bars = 10 μm. (E) Induction of NF-κB luciferase activity by muramyl dipeptide (MDP) via poNOD2. HEK293^{Cont} or HEK293^{poNOD2} cells were treated with the indicated concentrations of MDP for 24 h with or without pretreatment with cytochalasin D (CytoD, 1 μM) for 30 min. Values represent means and error bars indicate the standard deviation. The results are representative of three or four independent experiments. $^{*}P < 0.05$; $^{**}P < 0.01$ compared to cells treated with medium alone. (For interpretation of the references to colour in this figure legend, the reader is referred to the web version of the article.)

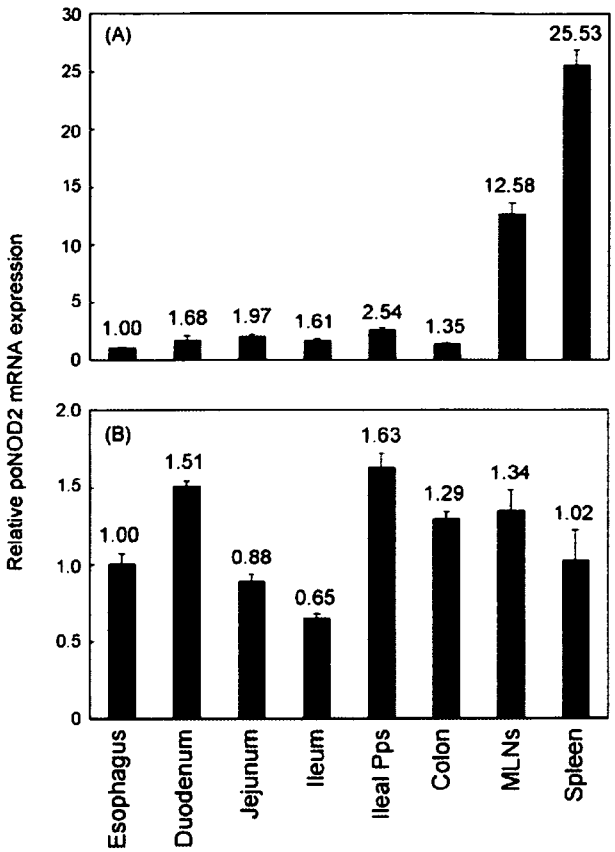

Fig. 4. NOD2 expression in swine tissues analysed by real-time quantitative PCR (A, newborn; B, adult). The poNOD2 mRNA level was normalized by the porcine β-actin mRNA, and the relative index was determined in comparison to the NOD2 mRNA level in esophagus (1.00). Values represent means and error bars indicate the standard deviation. The results are means of three independent experiments using tissues from at least three individual newborn or adult swine.

3.4. Upregulation of NOD2 expression by microbial stimulation in adult and newborn swine GALT

Host microflora interactions occur in the GALT including MLNs and Pps during postnatal periods. Several studies have demonstrated that microbial stimulation in the gut is important for the normal development of mucosal immunity after birth (Pollard and Sharon, 1970; Shaedler et al., 1965). To clarify the induction of NOD2 expression in GALT via TLRs and NOD2 signaling pathway, we analyzed the effects of various bacterial cell components on the expression of NOD2 in adult and newborn swine GALT, such as MLNs and Pps. In the present study, we used solely chemically synthesized PAMPs to avoid the effects of minor bioactive substances contaminating bacterial cell surface components prepared from bacteria. Namely, synthetic bacterial lipopeptide Pam3Cys is an agonist for TLR2, synthetic CpG DNA motif CpG2006-TGTT is an agonist for TLR9, MDP is an agonist for NOD2. In addition to these synthetic agonists, two strains of immunobiotic LAB, which are recognized by porcine TLR2 and TLR9 (Tohno et al., 2005a; Shimosato et al., 2006), were also used. For the individual ligands, titration studies were performed to determine the optimal concentration for the experimental systems (data not shown).

In the adult swine MLNs and Pps, MDP, Pam3Cys, CpG2006-TGTT and two strains of LAB induced significant increase in the levels of NOD2 gene transcripts at the 3 and 6 h (Fig. 5). In the immature ileal Pps and MLNs, these all ligands enhanced the expression of NOD2 at the time dependent manner, and significant upregulation was observed after a 6-h stimulation (Fig. 5). The induction level of NOD2 by the stimulation with TLRs and NOD2 ligands was higher in GALT of adults than in that of newborns, because the previous and present study revealed that adult swine GALT highly expresses TLR2, TLR9 and NOD2 than newborns GALT (Tohno et al., 2006). These results indicate that NOD2 expression is upregulated via signaling pathways mediated by TLR2, TLR9 and NOD2 in adult and newborn swine GALT where these receptors recognizes intestinal bacterial components. The mechanisms for NOD2 upregulation in the gut have not been fully elucidated. In the osteoblasts and astrocytes, it has been suggested that regulations in the amount of NOD2 protein may be secondary to signaling by pathogen-recognition molecules (Marriott et al., 2005; Sterka et al., 2006). Pro-inflammatory cytokines such as tumour-necrosis factor-α (TNF-α) and interferon-γ (IFN-γ) may play an important role in the induction of NOD2 gene (Rosenstiel et al., 2003). In our previous study, newborn and adult swine's GALT produce IFN-γ upon stimulation by CpG2006. (Tohno et al., 2006; Shimosato et al., 2006). IFN-γ production was also upregulated via TLR2-mediated signaling pathway (Tohno et al., 2006). Therefore, our current findings support the hypothesis that the ligands of TLR2 and TLR9 may enhance NOD2 expression through TLR2 and TLR9-promoted production of IFN-γ. Since NOD2 promoter contains NF-κB binding sites (Gutierrez et al., 2002; Rosenstiel et al., 2003), it is believed that TLRs and NOD2, as well as proinflamatory cytokine may upregulate NOD2 expression by activating NF-κB.

In our study, two strains of LAB, *L. gasseri* JCM1131^T and *L. bulgaricus* N1A1 B6 potently upregulated NOD2 expression in adult and newborn ileal Pps. Because M cells in Pps, which transport antigenic stimulants across epithelial barriers to initiate immune responses by lymphoid cells, express TLR2 and directly capture antigens across specialized follicle-associated epithelium (Tohno et al., 2006), intestinal bacteria including immunobiotic LAB may directly promotes the expression of NOD2 in the ileal Pps during postnatal development of the GALT, resulting in high level expression of NOD2 in adult GALT. In this context, oral vaccines and immunobiotic LAB contained in food may contribute to the development of NOD2 recognition in the mucosal immune system.

In conclusion, our cloning and characterization of poNOD2 gene revealed its localization not only in the cytoplasm but also in the inner side of the cell membrane. We also found that MDP potently activates NF-κB by interacting with poNOD2. Thus, NOD2 is an important immunoregulator in swine intestinal immunity. Furthermore, the expression pattern and regulation of NOD2 in newborn and adult swine may serve as a model system for studies of the development of human immune system.

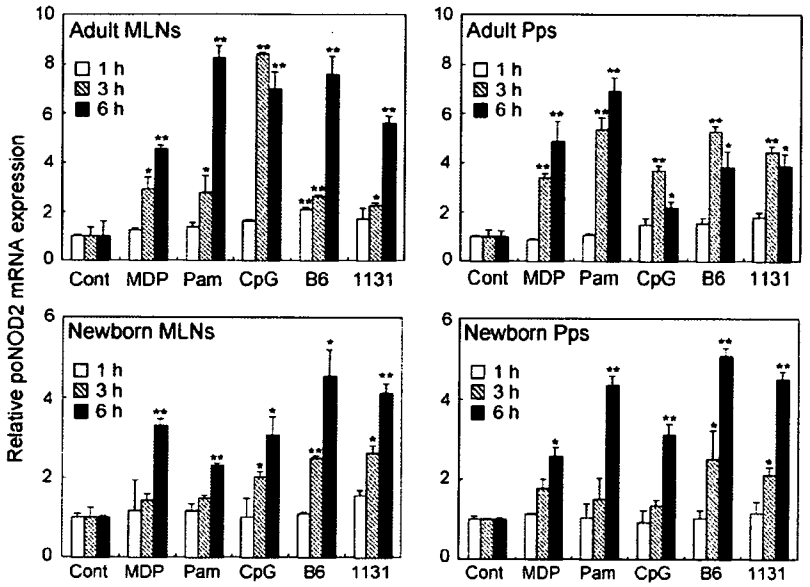

Fig. 5. Induction of NOD2 in MLNs and ileal Pps of adult and newborn swine. Cells (2×10^6 cells) from MLNs and ileal Pps were cultured in the absence (Cont) or presence of muramyl dipeptide (MDP; 50 μg/mL), Pam3Cys (Pam; 1ng/mL), CpG2006-TGTT (CpG; 1 μM), *Lactobacillus gasseri* JCM1131^T (1131; 100 μg/mL), or *Lactobacillus bulgaricus* NIAI B6 (B6; 100 μg/mL) for the indicated times. The expression of poNOD2 mRNA was determined by real-time PCR. Results are expressed as the relative mRNA index, calculated as the mRNA index (estimated poNOD2 mRNA copy number/estimated porcine β-actin mRNA copy number) of stimulated cells divided by the mRNA index of unstimulated cells. Columns represent the mean relative index, and error bars indicate the standard errors. Each experiment was repeated three times. $^{**}P<0.01$ and $^{*}P<0.05$ vs. cells cultured in the absence of stimulants.

Acknowledgements

We sincerely thank Dr. T. Shimosato (Section of Retroviral Immunology, Center for Biologics Evaluation Research, US Food and Drug Administration, USA) for helpful discussions and Dr. H. Inadera (Department of Public Health, Toyama Medical and Pharmaceutical University, Japan) for the kind gifts of the pGLM-ENH-luci vector. This study was partly supported by a Grant-in-Aid for Scientific Research (B)(2) (No., 18380158) from the Japan Society for the Promotion of Science, and NISR Research Grant from the Noda Institute for Scientific Research to Dr. H. Kitazawa, and the Secure and Healthy Animal Production project from the Ministry of Agriculture, Forestry and Fisheries of Japan to Dr. H. Aso and Dr. H. Kitazawa. M. Tohno is supported by JSPS research fellow (Research Fellowships for Young Scientists Program, No. 18005121). Dr. H. Kitazawa was supported by Program to Enhance International Standing of Higher Education in Japan 2006 (MEXT: Ministry of Education, Culture, Sports, Science and Technology).

References

Akira, S., Uematsu, S., Takeuchi, O., 2006. Pathogen recognition and innate immunity. Cell 124, 783–801.

Barnich, N., Aguirre, J.E., Reinecker, H.C., Xavier, R., Podolsky, D.K., 2005. Membrane recruitment of NOD2 in intestinal epithelial cells is essential for nuclear factor-{kappa}B activation in muramyl dipeptide recognition. J. Cell Biol. 170, 21–26.

Girardin, S.E., Boneca, I.G., Viala, J., Chamaillard, M., Labigne, A., Thomas, G., Philpott, D.J., Sansonetti, P.J., 2003. Nod2 is a general sensor of peptidoglycan through muramyl dipeptide (MDP) detection. J. Biol. Chem. 278, 8869–8872.

Gutierrez, O., Pipaon, C., Inohara, N., Fontalba, A., Ogura, Y., Prosper, F., Nunez, G., Fernandez-Luna, J.L., 2002. Induction of Nod2 in myelomonocytic and intestinal epithelial cells via nuclear factor-kappa B activation. J. Biol. Chem. 277, 41701–41705.

Inohara, N., Nunez, G., 2003. NODs: intracellular proteins involved in inflammation and apoptosis. Nat. Rev. Immunol. 3, 371–382.

Inohara, N., Ogura, Y., Fontalba, A., Gutierrez, O., Pons, F., Crespo, J., Fukase, K., Inamura, S., Kusumoto, S., Hashimoto, M., Foster, S.J., Moran, A.P., Fernandez-Luna, J.L., Nunez, G., 2003. Host recognition of bacterial muramyl dipeptide mediated through NOD2. Implications for Crohn's disease. J. Biol. Chem. 278, 5509–5512.

Magalhaes, J.G., Philpott, D.J., Nahori, M.A., Jehanno, M., Fritz, J., Bourhis, L.L., Viala, J., Hugot, J.P., Giovannini, M., Bertin, J., Lepoivre, M., Mengin-Lecreulx, D., Sansonetti, P.J., Girardin, S.E., 2005. Murine Nod1 but not its human orthologue mediates innate immune detection of tracheal cytotoxin. EMBO Rep. 6, 1201–1207.

Marriott, I., Rati, D.M., McCall, S.H., Tranguch, S.L., 2005. Induction of Nod1 and Nod2 intracellular pattern recognition receptors in murine osteoblasts following bacterial challenge. Infect. Immun. 73, 2967–2973.

Medzhitov, R., Janeway Jr., C., 2000. Innate immune recognition: mechanisms and pathways. Immunol. Rev. 173, 89–97.

Meylan, E., Tschopp, J., Karin, M., 2006. Intracellular pattern recognition receptors in the host response. Nature 442, 39–44.

Piguet, P.F., Irle, C., Vassalli, P., 1981. Immunosuppressor cells from newborn mouse spleen are macrophages differentiating in vitro from monoblastic precursors. Eur. J. Immunol. 11, 56–61.

Pollard, M., Sharon, N., 1970. Responses of the Peyer's Patches in Germ-Free Mice to Antigenic Stimulation. Infect. Immun. 2, 96–100.

Rosenstiel, P., Fantini, M., Brautigam, K., Kuhbacher, T., Waetzig, G.H., Seegert, D., Schreiber, S., 2003. TNF-alpha and IFN-gamma regulate the expression of the NOD2 (CARD15) gene in human intestinal epithelial cells. Gastroenterology 124, 1001–1009.

Saitou, N., Nei, M., 1987. The neighbor-joining method: a new method for reconstructing phylogenetic trees. Mol. Biol. Evol. 4, 406–425.

Schultz, J., Copley, R.R., Doerks, T., Ponting, C.P., Bork, P., 2000. SMART: a web-based tool for the study of genetically mobile domains. Nucl. Acids Res. 28, 231–234.

Shaedler, R.W., Dubos, R., Costello, R., 1965. Association of germ-free mice with bacteria isolated from normal mice. J. Exp. Med. 122, 77–93.

Shimosato, T., Kitazawa, H., Katoh, S., Tomioka, Y., Karima, R., Ueha, S., Kawai, Y., Hishinuma, T., Matsushima, K., Saito, T., 2003. Swine Toll-like receptor 9 recognizes CpG motifs of human cell stimulant. Biochim. Biophys. Acta 1627, 56–61.

Shimosato, T., Kitazawa, H., Tohno, M., Katoh, S., Kawai, Y., Saito, T., 2004. Development of immune assay system for both CpG and non-CpG DNA from lactic acid bacteria using a transfectant of swine Toll-like receptor 9. Anim. Sci. J. 75, 377–382.

Shimosato, T., Kitazawa, H., Katoh, S., Tohno, M., Iliev, I.D., Nagasawa, C., Kimura, T., Kawai, Y., Saito, T., 2005a. Augmentation of T(H)-1 type response by immunoactive AT oligonucleotide from lactic acid bacteria via Toll-like receptor 9 signaling. Biochem. Biophys. Res. Commun. 326, 782–787.

Shimosato, T., Tohno, M., Kitazawa, H., Katoh, S., Watanabe, K., Kawai, Y., Aso, H., Yamaguchi, T., Saito, T., 2005b. Toll-like receptor 9 is expressed on follicle-associated epithelia containing M cells in swine Peyer's patches. Immunol. Lett. 98, 83–89.

Shimosato, T., Kimura, T., Tohno, M., Iliev, I.D., Katoh, S., Ito, Y., Kawai, Y., Sasaki, T., Saito, T., Kitazawa, H., 2006. Strong immunostimulatory activity of AT-oligodeoxynucleotide requires a six-base loop with a self-stabilized 5′-C···G-3′ stem structure. Cell. Microbiol. 8, 485–495.

Sterka Jr., D., Rati, D.M., Marriott, I., 2006. Functional expression of NOD2, a novel pattern recognition receptor for bacterial motifs, in primary murine astrocytes. Glia 53, 322–330.

Strober, W., Murray, P.J., Kitani, A., Watanabe, T., 2006. Signalling pathways and molecular interactions of NOD1 and NOD2. Nat. Rev. Immunol. 6, 9–20.

Sugawara, Y., Uehara, A., Fujimoto, Y., Kusumoto, S., Fukase, K., Shibata, K., Sugawara, S., Sasano, T., Takada, H., 2006. Toll-like receptors, NOD1, and NOD2 in oral epithelial cells. J. Dent. Res. 85, 524–529.

Thompson, J.D., Higgins, D.G., Gibson, T.J., 1994. Clustal W: improving the sensitivity of progressive multiple sequence alignment through sequence weighting, position-specific gap penalties and weight matrix choice. Nucl. Acids Res. 22, 4673–4680.

Tohno, M., Kitazawa, H., Shimosato, T., Matsumoto, M., Katoh, S., Kawai, Y., Saito, T., 2005a. A swine toll-like receptor 2-expressing transfectant as a potential primary screening system for immunobiotic microorganisms. FEMS Immunol. Med. Microbiol. 44, 283–288.

Tohno, M., Shimosato, T., Kitazawa, H., Katoh, S., Iliev, I.D., Kimura, T., Kawai, Y., Watanabe, K., Aso, H., Yamaguchi, T., Saito, T., 2005b. Toll-like receptor 2 is expressed on the intestinal M cells in swine. Biochem. Biophys. Res. Commun. 330, 547–554.

Tohno, M., Shimosato, T., Moue, M., Aso, H., Watanabe, K.; Kawai, Y., Yamaguchi, T., Saito, T., Kitazawa, H., 2006. Toll-like receptor 2 and 9 are expressed and functional in gut-associated lymphoid tissues of presuckling newborn swine. Vet. Res. 37, 1–22.

Tohno, M., Shimazu, T., Ueda, W., Anzawa, D., Aso, H., Nishimura, J., Kawai, Y., Saito, Y., Saito, T., Kitazawa, H., 2007a. Molecular cloning of porcine RP105/MD-1 involved in recognition of extracellular phosphopolysaccharides from *Lactococcus lactis* ssp. *cremoris*. Mol. Immunol. 44, 2566–2577.

Tohno, M., Shimosato, T., Kawai, Y., Aso, H., Ikegami, H., Taketomo, N., Saito, T., Kitazawa, H., 2007b. Advanced molecular immunoassay system for immunobiotic lactic acid bacteria using a transfectant of Toll-like receptor 2. Anim. Sci. J. 78, 195–205.

Uchiyama, T., Kulkarni, A.A., Davies, D.L., Lee, V.H., 2003. Biophysical evidence for His57 as a proton-binding site in the mammalian intestinal transporter hPepT1. Pharm. Res. 20, 1911–1916.

Ueda, A., Ishigatsubo, Y., Okubo, T., Yoshimura, T., 1997. Transcriptional regulation of the human monocyte chemoattractant protein-1 gene. Cooperation of two NF-kappaB sites and NF-kappaB/Rel subunit specificity. J. Biol. Chem. 272, 31092–31099.

Uehara, A., Fujimoto, Y., Kawasaki, A., Kusumoto, S., Fukase, K., Takada, H., 2006. Meso-diaminopimelic acid and meso-lanthionine, amino acids specific to bacterial peptidoglycans, activate human epithelial cells through NOD1. J. Immunol. 177, 1796–1804.

Vavricka, S.R., Musch, M.W., Chang, J.E., Nakagawa, Y., Phanvijhitsiri, K., Waypa, T.S., Merlin, D., Schneewind, O., Chang, E.B., 2004. hPepT1 transports muramyl dipeptide, activating NF-kappaB and stimulating IL-8 secretion in human colonic Caco2/bbe cells. Gastroenterology 127, 1401–1409.

Viala, J., Chaput, C., Boneca, I.G., Cardona, A., Girardin, S.E., Moran, A.P., Athman, R., Memet, S., Huerre, M.R., Coyle, A.J., DiStefano, P.S., Sansonetti, P.J., Labigne, A., Bertin, J., Philpott, D.J., Ferrero, R.L., 2004. Nod1 responds to peptidoglycan delivered by the Helicobacter pylori cag pathogenicity island. Nat. Immunol. 5, 1166–1174.

Wang, Z.M., Li, X., Cocklin, R.R., Wang, M., Wang, M., Fukase, K., Inamura, S., Kusumoto, S., Gupta, D., Dziarski, R., 2003. Human peptidoglycan recognition protein-L is an *N*-acetylmuramoyl-L-alanine amidase. J. Biol. Chem. 278, 49044–49052.

Available online at www.sciencedirect.com
ScienceDirect
Molecular Immunology 45 (2008) 1807–1817
Molecular Immunology
www.elsevier.com/locate/molimm

Molecular cloning and functional characterization of porcine nucleotide-binding oligomerization domain-1 (NOD1) recognizing minimum agonists, *meso*-diaminopimelic acid and *meso*-lanthionine

Masanori Tohno[a], Tomoyuki Shimazu[a], Hisashi Aso[b], Akiko Uehara[c], Haruhiko Takada[c], Akiko Kawasaki[d], Yukari Fujimoto[d], Koichi Fukase[d], Tadao Saito[a], Haruki Kitazawa[a,*]

[a] *Food Immunology Group, Laboratory of Animal Products Chemistry, Graduate School of Agricultural Science, Tohoku University, Aobaku, Sendai 981-8555, Japan*
[b] *Laboratory of Functional Morphology, Graduate School of Agricultural Science, Tohoku University, Aobaku, Sendai 981-8555, Japan*
[c] *Department of Microbiology and Immunology, Graduate School of Dentistry, Tohoku University, Aobaku, Sendai 980-8575, Japan*
[d] *Department of Chemistry, Graduate School of Science, Osaka University, Toyonaka, Osaka 560-0043, Japan*

Received 10 September 2007; received in revised form 22 September 2007; accepted 22 September 2007
Available online 5 November 2007

Abstract

In this study, we isolated a complementary DNA encoding nucleotide-binding oligomerization domain-1 (NOD1) from Peyer's patches (Pps) of swine gut-associated lymphoid tissues (GALT). The complete open reading frame of porcine NOD1 contains 2862 bp, encoding a 953-amino acid polypeptide. The porcine NOD1 amino acid sequence is more closely related to the human sequence (83.8% identity) than the mouse counterpart (79.2% identity). To examine the subcellular expression and function of porcine NOD1, we overexpressed it in human embryonic kidney 293 cells. Immunostaining with an anti-porcine NOD1 polyclonal antibody revealed that the protein was expressed in transfectants as an intracellular membrane-bound molecule. In the transfected cells, both γ-D-glutamyl-*meso*-diaminopimelic acid, and *meso*-diaminopimelic acid and *meso*-lanthionine activated nuclear factor-kappa B. Quantitative real-time PCR detected NOD1 mRNA in multiple tissues isolated from adult and newborn swine, including the esophagus, duodenum, jejunum, ileum, ileal Pps, colon, spleen, and mesenteric lymph nodes. In the newborn and adults, NOD1 was highly expressed in the esophagus and GALT, such in the ileal Pps and mesenteric lymph nodes. Furthermore, Toll-like receptor and NOD1 ligands as well as immunobiotic lactic acid bacteria enhanced the expression of NOD1 in GALT of adult and newborn swine. Our results should help clarify how the intestinal immune system is modulated by low-molecular weight peptidoglycan fragments through NOD1.

Keywords: NOD1; cDNA cloning; Swine; GALT; *meso*-DAP; *meso*-Lanthionine

1. Introduction

Peptidoglycan (PGN) is an essential component of cell walls of Gram-positive and Gram-negative bacteria (Myhre et al., 2006). PGN consists of a glycan backbone with alternating moieties of β(1–4)-linked *N*-acetylglucosamine acid and *N*-acetyl muramic acid, where muramic acid acts as a linker between sugars and stem peptides containing four alternating L- and D-amino acids. The initial amino acid of these tetrapeptides is an L-alanine, and the second and fourth amino acids are D-glutamine and D-alanine, respectively. In most Gram-positive bacteria, the third amino acid is L-lysine, whereas in most Gram-negative and some Gram-positive bacilli, it is *meso*-diaminopimelic acid (*meso*-DAP).

The minimal structure of PGN in Freund's complete adjuvant for stimulating cell-mediated immunity is muramyldipeptide (MDP; *N*-acetylmuramyl-L-alanyl-D-isoglutamine) (Ellouz et al., 1974; Kotani et al., 1975). MDP has also been reported to exhibit some of the immunobioactivities of PGN (Takada and Kotani, 1985, 1995). Desmuramylpeptides (DMPs) are another type of synthetic low-molecular weight PGN fragment that has similar immunobioactivities as MDP (Adam, 1985; Goto and

* Corresponding author. Tel.: +81 22 717 8713; fax: +81 22 717 8715.
E-mail address: haruki@bios.tohoku.ac.jp (H. Kitazawa).

0161-5890/$ – see front matter © 2007 Elsevier Ltd. All rights reserved.
doi:10.1016/j.molimm.2007.09.029

Aoki, 1987). Synthetic DMPs are analogous to PGN in that they both contain *meso*-DAP. Kitaura et al. (1982) reported that γ-D-glutamyl-*meso*-DAP (iE-DAP) is the minimum structural unit in the structure of DMPs necessary for eliciting immunological activities.

Recent studies have shown that a cytosolic surveillance system mediated by the nucleotide oligomerization domain (NOD) proteins plays an important role in recognizing intracellular pathogen-associated molecular patterns (PAMPs) (Meylan et al., 2006). NOD2 was identified as an intracellular receptor for MDP (Girardin et al., 2003a; Inohara et al., 2003). It has since been found that DAP-containing peptide moieties are recognized by NOD1. Furthermore, iE-DAP was sufficient for NOD1 activation, suggesting that it is the minimal structure recognized by NOD1 (Chamaillard et al., 2003; Girardin et al., 2003b). NOD1 and NOD2 mediate activation of mitogen-activated protein kinases and nuclear factor-kappa B (NF-κB) through the CARD-dependent recruitment of RIP2 (Inohara and Nuñez, 2003; Viala et al., 2004).

In recent years, there has been a growing interest in the swine immune system because of its possible use as a model for the human immune system and because of the economic importance of swine as livestock (Shimosato et al., 2005a; Tohno et al., 2005a). In addition, the structure of the human digestive system is more similar to that of swine than those of rodents. In our previous study, we cloned some porcine Toll-like receptor (TLR) family members as well as porcine NOD2, and we analyzed their tissue expression and the specificity of their ligands (Shimosato et al., 2003, 2005b; Tohno et al., 2005b, 2007a, 2008); however, the cellular and molecular mechanisms underlying NOD1 recognition of PAMPs in the swine immune system remain to be elucidated. Therefore, in the present study, we cloned porcine NOD1 (poNOD1) cDNA from ileal Peyer's patches (Pps) of adult swine. We constructed a cell line transfected with poNOD1 to investigate its function, especially in the recognition of various chemically synthesized low-molecular weight PGN fragments. In addition, we examined the expression of poNOD1 in diverse tissues from adult and newborn swine and analyzed the capacity of PAMPs and immunobiotic lactic acid bacteria to regulate the expression of poNOD1 in gut-associated lymphoid tissues (GALT) of adult and newborn swine.

2. Materials and methods

2.1. Experimental tissues

Experimental tissues (esophagus, duodenum, jejunum, ileum, ileal Pps, colon, spleen, and mesenteric lymph nodes [MLNs]) were obtained from newborn (before taking colostrum) and adult (1 year old) LWD swine (genotype 1/2 Duroc, 1/4 Landrace, 1/4 Large White; Hiruzu Co. Ltd., Miyagi, Japan) as described previously (Tohno et al., 2006, 2008). The swine used in experiments were clinically healthy and free of infectious diseases. All procedures were conducted in accordance with the Guidelines for Animal Experimentation of Tohoku University, Japan.

2.2. Stimulants

Synthetic MDP was purchased from Invivogen (San Diego, CA, USA), and iE-DAP was synthesized as previously described (Chamaillard et al., 2003). Synthetic DMP, FK156 (D-lactoyl-L-Ala-D-Glu-*meso*-DAP-Gly), and its derivative, FK565 (heptanoyl-D-Glu-*meso*-DAP-D-Ala) (Kitaura et al., 1982), was supplied by Astellas Pharmaceutical (formerly Fujisawa and Yamanouchi). *meso*-Lanthionine was synthesized by coupling of *N*-benzyloxycarbonyl-D-cysteine with L-chloroalanine as described by Photaki et al. (1979). Commercial DAP, which was a mixture of *meso*-DAP, LL-DAP, and DD-DAP, was obtained from Sigma (Tokyo, Japan), and *meso*-DAP, LL-DAP, and DD-DAP were prepared from the commercial DAP as previ-

Table 1
Primer sequences used in this study

Porcine NOD1 gene cloning primer	Sense primer	Antisense primer	Reference
Porcine NOD1 (109–773)	ACTCAGTGTCTGGTGGACAA	TAGTGCTTGAAGAGCAGGTC	
Porcine NOD1 (711–1434)	CATGTTCAGCTGCTTCAAGG	GAAAAGGAAGAGGCTCCTTCT	
Porcine NOD1 (1285–1777)	ACTGAGGTCCATCTGAACAG	ACAGGAAGAGGTTGGTGAAC	
Porcine NOD1 (1732–2360)	CCCTTCAAGAACAAGGACCA	TGAGGCCTTTGCATTCATCC	
Porcine NOD1 (2297–2719)	ACCAGATCACTGATGTCGGA	GATT CT GGAT CAGCCAT A AAT GC	
Porcine NOD1 (5′RACE, cDNA synthesized)		TGAGGTCCACGTAAGCATCT	
Porcine NOD1 (5′RACE, first nested PCR)	5′RACE Abridged Anchor Primer	GAAGACGAAGAACTCCGACA	
Porcine NOD1 (5′RACE, second nested PCR)	Abridged Universal Amplification Primer	GAAGTAGTCGTTGTGCAGCA	
Porcine NOD1 (3′RACE, cDNA synthesized)		Oligo-d(T)17 Adapter Primer	
Porcine NOD1 (3′RACE, first nested PCR)	CCTGCAGCAGAATGCGTCTCTGAGAA	Abridged Universal Amplification Primer	
Porcine NOD1 (3′RACE, 2st nested PCR)	CGAAGTGGCAGAGAGCTTAGCAGAGA	Abridged Universal Amplification Primer	
RT-PCR			
Human β-actin	GGATGCAGAAGGAGATCACTG	CGATCCACACGGAGTACTTG	Shimosato et al. (2005b)
Porcine NOD1	CTCTGAGAATATTCTGGCTC	GTGTTGTTCTGTAAGGCATC	In this study
Real-time PCR			
Porcine β-actin	CATCACCATCGGCAACGA	GCGTAGAGGTCCTTCCTGATGT	Tohno et al. (2006)
Porcine NOD1	CTGTCGTCAACACCGATCCA	CCAGTTGGTGACGCAGCTT	In this study

5′RACE Abridged Anchor Primer, Abridged Universal Amplification Primer and Oligo-d(T)17 Adaptor Primer were purchased from Invitrogen.

ously described (Uehara et al., 2006). The synthetic bacterial lipopeptide Pam3Cys was obtained from EMC Microcollection (Tübingen, Germany). CpG DNA motif CpG2006-TGTT was synthesized by Operon (Tokyo, Japan; Shimosato et al., 2006). Two bacterial species, *L. delbrueckii* ssp. *bulgaricus* and *L. gasseri*, were also tested in the present study. *Lactobacillus* (*L.*) *bulgaricus* N1A1 B6 was obtained from the National Institute of Animal Industry (Tukuba, Japan). *L. gasseri* JCM1131^T was purchased from the Japan Collection of Microorganisms RIKEN BioResource Center (Saitama, Japan). All strains were cultured at 37 °C for 16 h in Man Rogosa Sharpe broth (Difco, Detroit, USA), washed, and lyophilized for further analysis.

2.3. Cloning of poNOD1

Total RNA was isolated from adult ileal Pps using an RNeasy Protect Starter Kit (Qiagen, Tokyo, Japan) as previously described (Shimosato et al., 2003). Primers were synthesized with the sequences deduced from alignment of conserved sequences for human (accession no. NM_006092) and mouse NOD1 (accession no. NM_172729) (Table 1). These primers along with Thermoscript reverse transcriptase (Invitrogen, Carlsbad, CA, USA) were used to synthesize the first-strand cDNA from the total RNA. The PCR products were subcloned into the vector pGEM-T easy DNA (Promega, Madison, WI, USA). The 5′- and 3′-flanking regions of poNOD1 were determined with a 5′- and 3′-RACE system for rapid amplification of cDNA ends (Invitrogen). DNA sequencing was performed using an ABI310 Sequence-Analyzer (Applied Biosystems, Foster City, CA, USA). GENETYX-SV/RC Ver.13.0.6 software (GENETYX Co., Tokyo, Japan) was used to analyze nucleotide and deduced amino acid sequences. The SMART architecture research program (http://smart.embl-heidelberg.de/) was used for the identification and annotation of protein domains.

2.4. Polyclonal antibody to poNOD1

The poNOD1 protein was analyzed using GENETYX-SV/RC Ver.13.0.6 to predict secondary structure, hydrophobicity, and antigenicity. Based on this analysis, a 13-amino acid sequence (FHDAFDSSLQLPD; residues 404–416) was chosen for antigen peptide synthesis. Synthetic polypeptides with an added cysteine at the N-terminus were emulsified in an equal volume of Freund's Complete Adjuvant. The anti-poNOD1 polyclonal antibody was generated by immunizing Japanese white rabbits with synthetic polypeptides at a dose of 0.3 mg per rabbit. After two boosters at monthly intervals, the rabbits were bled, and the antisera were collected and purified by epitope affinity chromatography. Finally, high antibody titers for poNOD1 were identified by a direct enzyme-linked immunosorbent assay (data not shown).

2.5. Cells

Human embryonic kidney (HEK) 293 cells were obtained from the TKG cell bank (Institute of Development, Aging and Cancer, Tohoku University, Sendai, Japan) and were maintained in complete Dulbecco's modified Eagle's medium (Sigma) supplemented with 10% fetal calf serum (Hyclone, Logan, UT, USA), 50 mg/mL penicillin/streptomycin, 2 mM L-glutamine, 10 mM 2-[4-(2-hydroxyethyl)-1-piperadinyl] ethansulfonic acid, 0.11 mg/mL sodium pyruvate, and 0.5 mM 2-mercaptoethanol (Sigma).

2.6. Transfection

HEK293 cells were transfected with plasmids according to our previous reports (Tohno et al., 2005b, 2008). Briefly, the cells (4×10^5 per well) were plated in six-well plates 24 h prior to transfection. The cells were transfected with the pcDNA3 vector (Invitrogen) encoding C-terminally FLAG-tagged poNOD1 (5 μg/well) using Lipofectamine™ LTX and Plus™ Reagent (Invitrogen). The expression of poNOD1 was confirmed by intracellular staining with an anti-FLAG M2 monoclonal antibody (Sigma) and an anti-poNOD1 polyclonal antibody. To construct non-tagged transfectants, the cells were transiently transfected with the pcDNA vector encoding non-tagged poNOD1. Transfectants expressing poNOD1-FLAG were designated HEK293^{poNOD1}, and HEK293 cells transfected with control plasmid vector were designated HEK293^{Cont}.

2.7. Analysis of poNOD1 expression

First, cDNA was synthesized from total RNA prepared from the HEK293 cells using TRIZOL reagent (Invitrogen) and amplified using ExTaq polymerase (TaKaRa Bio Inc., Otsu, Japan) as previously described (Shimosato et al., 2004; Tohno et al., 2007b). The primers used for reverse transcription (RT)-PCR are listed in Table 1. The expression of β-actin was used as a control. PCR products were separated by electrophoresis on 1.5% agarose gels and visualized by ethidium bromide staining.

For protein expression, flow cytometry was conducted as described (Tohno et al., 2008). Briefly, HEK293^{poNOD1} cells were stained using anti-FLAG or anti-poNOD1. After washing with phosphate buffered saline (PBS) containing 2% fetal calf serum, the cells were treated with phycoerythrin-conjugated anti-mouse IgG (Sigma) or Alexa488-conjugated anti-rabbit IgG (Invitrogen). The phycoerythrin or Alexa488 signal was measured by flow cytometry using a FACSCalibur™ (Becton Dickinson, Tokyo, Japan). Permeabilized cells were stained in a staining buffer containing 0.1% saponin (Sigma). Extracellular staining was also conducted using a staining buffer without saponin. HEK293^{Cont} or HEK293^{poNOD1} stained with the secondary antibody only served as negative controls. Both negative controls showed low levels of background fluorescence.

Confocal laser scanning microscopy was performed (Tohno et al., 2008) by growing cells on glass coverslips followed by washing with PBS and fixation with 2% paraformaldehyde containing 0.1% Triton X-100 at 4 °C for 30 min. For cell surface staining, the cells were fixed with 2% paraformaldehyde at 4 °C for 30 min. After three washes with PBS, the cells were stained with anti-FLAG M2 monoclonal antibody followed by Alexa 647-conjugated anti-mouse IgG (Invitrogen). The non-tagged poNOD1-expressing transfectants were stained

with anti-poNOD1 polyclonal antibody followed by Alexa 488-conjugated anti-rabbit IgG. All cells were protected from direct light exposure and were washed three times with PBS and then stained with SYTOX orange (Invitrogen) to detect nuclei. Finally, the cells were washed three times with PBS, immersed in PermaFluor aqueous mounting reagent (Immunon, Pittsburgh, PA, USA), and observed under a MRC-1024 confocal laser microscope (Bio-Rad, Richmond, CA, USA).

2.8. NF-κB reporter luciferase assay

HEK293^{Cont} or HEK293^{poNOD1} cells (8×10^4 per well in a 24-well plate) were transfected for 4 h using Lipofectamine™ reagent with pGLM-ENH-luci vector (Shimosato et al., 2006). After a 24-h stimulation with various concentrations of the indicated low-molecular weight PGN fragments, luciferase levels were measured according to the manufacturer's protocol (Promega, Tokyo, Japan). In some experiments, cytochalasin D (1 μM) was added directly to the cell culture medium for 30 min to enhance the stimulation by PGN fragments without toxic effects on the cells (Magalhaes et al., 2005; Uehara et al., 2006; Tohno et al., 2008). The relative index was estimated from the resonance units (RU) using the following equation: relative Index = [(RU in stimulated cultures) − (RU in background)]/[(RU in non-stimulation) − (RU in background)]. All assays were conducted at least three times in triplicate.

2.9. Real-time quantitative PCR

Total RNA was isolated from various adult and newborn swine tissues as described (Tohno et al., 2006). Briefly, cDNAs were prepared by RT of 1 μg total RNA using QuantiTect Reverse Transcription Kit (Qiagen). An equivalent volume of cDNA solution from each sample was used for quantification of poNOD1-specific cDNA by real-time quantitative PCR. The reactions occurred on a 7300 Real Time PCR System (Applied Biosystems) using Platinum SYBR Green qPCR SuperMix UDG with ROX (Invitrogen) and the primers listed in Table 1. The results are expressed as the relative mRNA index, calculated as the index (NOD1 mRNA copy number/β-actin mRNA copy number) for the test sample divided by the index in the esophagus. In the control tubes, poly $(A)^+$ RNA samples were used as templates to examine the presence of contaminating genomic DNA. Amplification products of contaminants such as primer dimers were not detected by SYBR green chemistry using serial dilutions of cDNA. DNA sequencing confirmed that the amplified cDNAs were identical to bases 356 to 412 of poNOD1.

2.10. Measurement of NOD1 expression

Single-cell suspensions from ileal Pps and MLNs were prepared as previously described (Tohno et al., 2006). Total RNA was isolated from 2×10^6 ileal Pps and MLNs cells treated with MDP (1, 10, 50 μg/mL), iE-DAP (1, 10, 50 μg/mL), CpG2006-TGTT (0.1, 1, 5 μM), Pam3Cys (0.1, 1, 10 ng/mL), *L. gasseri* JCM1131^T (1, 10, 100 μg/mL), or *L. bulgaricus* NIAI B6 (1, 10, 100 μg/mL) for the indicated times at 37 °C in 5% CO_2. Three replicates were prepared for each condition. The isolated RNA samples were then converted to cDNA by RT and then used for real-time PCR (see Section 2.9).

2.11. Statistics

All results represent the average of three to five separate experiments. The statistical significance of differences was assessed using Student's *t*-test.

3. Results

3.1. Cloning and characterization of poNOD1

The cDNA encoding poNOD1 was derived from mRNA isolated from adult swine ileal Pps. The sequences were confirmed in ileal Pps from three different swine. Nucleotide sequencing of poNOD1 revealed a 3599-bp cDNA sequence including the poNOD1 structural gene. The predicted open reading frame lies between nucleotides 338 and 3199 and encodes a 953-amino acid protein (Fig. 1A). Analysis of the primary structure of poNOD1 using the SMART architecture research program identified no signal peptide, multiple C-terminal LRR domains, a central NACHT domain, and an N-terminal CARD domain (Fig. 1B).

Comparison of the nucleic acid sequences for the open reading frame of poNOD1 with those of human and mouse NOD1 indicated 86.7% and 80.9% identity, respectively. At the deduced amino acid level, the corresponding identities were 83.8% and 79.2%, respectively. In the phylogenetic analysis, poNOD1 belonged to the group containing human, chimpanzee, and rhesus monkey NOD1 (Supplementary Fig. 1).

3.2. Subcellular localization of poNOD1

To clarify the subcellular expression pattern of poNOD1, we established poNOD1-expressing HEK293 (HEK293^{poNOD1}) cells. RT-PCR analysis revealed that the mRNA for poNOD1 was present only in the HEK293^{poNOD1} cells (Fig. 2A). Intracellular staining of HEK293^{poNOD1} cells with an anti-FLAG antibody or an anti-poNOD1 antibody, followed by flow cytometric analysis showed that only HEK293^{poNOD1} cells were FLAG-poNOD1-positive (Fig. 2B). Extracellular staining clearly showed that FLAG-poNOD1 was not expressed on the cell surface (Fig. 2B). Similarly, confocal laser microscopy indicated that poNOD1 was not on cell surface (Fig. 2C, c) but was present in the intracellular compartment (Fig. 2C, d) and located close to the plasma membrane (Fig. 2C, d arrows). No extracellular or intracellular expression of poNOD1 was observed in HEK293^{Cont} cells (Fig. 2C, a and b).

To confirm that the FLAG-tag did not cause the membrane association, wild-type poNOD1 lacking the FLAG-tag was transiently overexpressed in HEK293 cells. Intracellular immunostaining of non-tagged poNOD1-expressing cells with an anti-poNOD1 antibody revealed that poNOD1 was localized in the cytosol and also was enriched in areas close to the cell membrane (Fig. 2D, arrows), indicating that the FLAG-tag

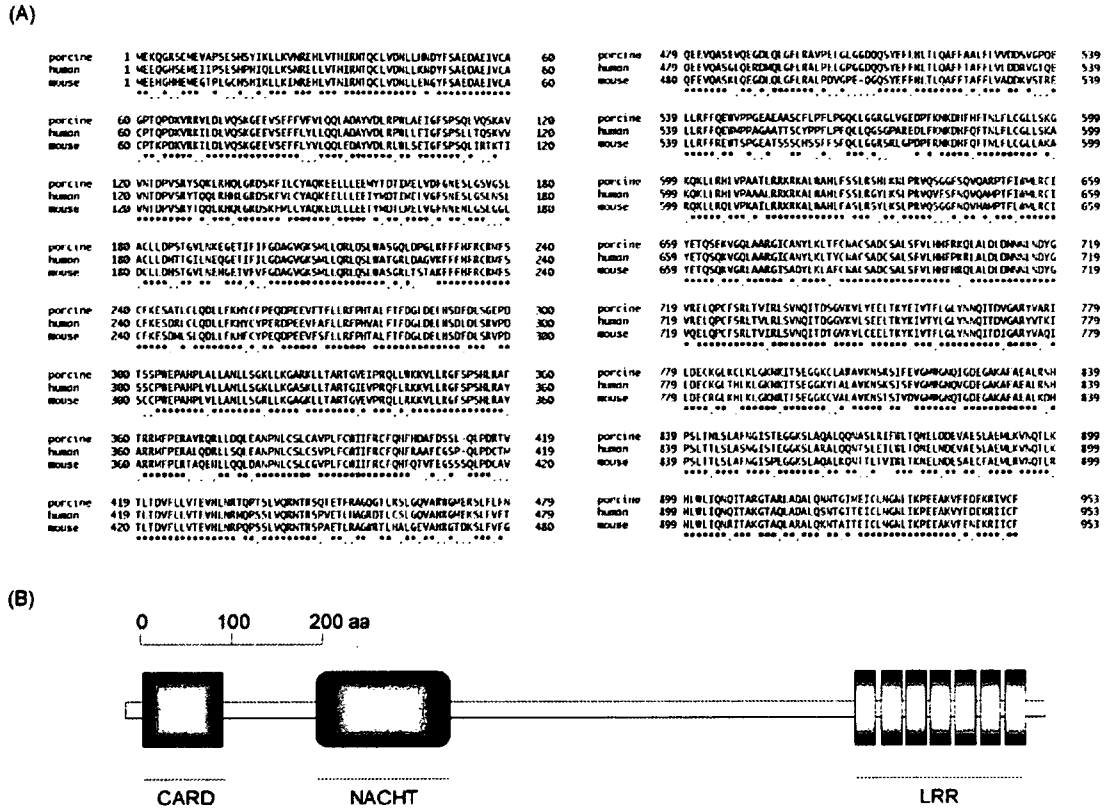

Fig. 1. Alignment and architecture of the deduced amino acid sequences for NOD1. (A) Alignment of the amino acid sequences of porcine, human, and mouse NOD1. The numbers indicate the amino acid position. Identical amino acid residues are marked with asterisks, and similar residues are marked with dots. Gaps were introduced to optimize alignment. (B) Architecture of poNOD1. The protein sequence of poNOD1 was analyzed using SMART. CARD, caspase recruitment domain; NACHT domain The nucleotide sequence of poNOD1 has been submitted to the DDBJ, EMBL, and GenBank nucleotide databases under accession number AB187219.

did not affect cellular localization of poNOD-1. These results confirm that the cloned poNOD1 was expressed only in the intracellular regions and associated with the intracellular side of the cell membrane. Furthermore, real-time PCR analysis showed that the expression of human NOD1 and NOD2 was not altered in the HEK293^{poNOD1} and HEK293^{Cont} during the transfection process (data not shown).

3.3. Recognition of PGN fragments by poNOD1

To determine which PGN fragments are recognized by poNOD1, we stimulated HEK293^{poNOD1} cells with various low-molecular weight PGN fragments (iE-DAP, FK156, FK565, DAP, and MDP) and evaluated the activation of NF-κB. When stimulated by iE-DAP, there was a significant increase in NF-κB-dependent luciferase activity in HEK293^{poNOD1} cells (Fig. 3A). When the HEK293^{poNOD1} cells were stimulated with DMPs such as FK156 and FK565, there was also a marked and dose-dependent activation of NF-κB (Fig. 3A). In addition, iE-DAP caused a higher level of NF-κB activation than FK156 and FK565 in the HEK293^{poNOD1} cells. Furthermore, high concentrations of a commercial DAP containing three stereoisomers of DAP significantly enhanced the activity of NF-κB in HEK293^{poNOD1} cells.

We also found that cytochalasin D enhanced the activation of NF-κB in.HEK293^{poNOD1} (Fig. 3B). However, MDP, a ligand for NOD2, did not stimulate NF-κB in HEK293^{poNOD1} cells in the presence or absence of cytochalasin D (Fig. 3A and B). Similar responses were observed in cells transiently expressing non-tagged poNOD1 (data not shown). Finally, in the presence or absence of cytochalasin D, all tested PGN fragments were inactive in HEK293^{Cont} cells (Fig. 3A and B). These findings suggest that, when expressed in HEK293 cells, the cloned poNOD1 is functional and recognizes iE-DAP and DMPs, resulting in the activation of NF-κB. Furthermore, we showed for the first time that DAP itself can activate NF-κB through the poNOD1 signaling pathway.

3.4. poNOD1 recognizes meso-DAP and meso-lanthionine

Because the commercial DAP is a mixture of three stereoisomers (LL-, DD- and *meso*-), we chemically synthesized and purified the individual isomers to identify which was the active isomer(s) sufficient for activation of the poNOD1 signaling pathway. We performed titration studies to determine the optimal concentration of the individual ligands for the experimental systems (data not shown). As shown in Fig. 4A,

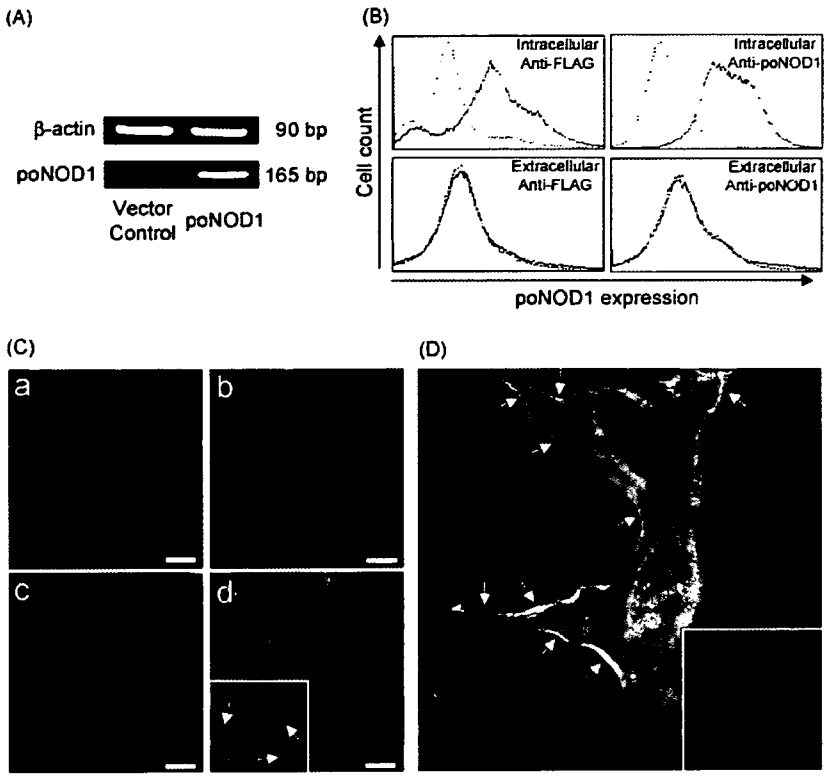

Fig. 2. Analysis of poNOD1 expression in HEK293 cells. (A) The expression of poNOD1 mRNA in HEK293^{poNOD1} cells was analyzed by RT-PCR. The PCR products were detected by agarose gel electrophoresis followed by staining with ethidium bromide. (B) The expression of poNOD1-FLAG protein in HEK293^{poNOD1} cells was detected by intracellular or extracellular staining with phycoerythrin-conjugated anti-FLAG monoclonal antibody or Alexa488-conjugated anti-poNOD1 polyclonal antibody followed by flow cytometry. Solid and dotted lines indicate HEK293^{poNOD1} and vector control cells, respectively. (C) Cellular localization of poNOD1 was observed by confocal laser microscopy: shown are (a) cell surface, (b) intracellular staining of HEK293^{Cont} cells, (c) cell surface and (d) intracellular staining of HEK293^{poNOD1} cells with anti-FLAG monoclonal antibody, followed by Alexa 647-conjugated anti-mouse IgG (blue). Nuclei were stained with SYTOX orange (red). Representative sections from one of six independent experiments are shown. Scale bars = 50 μm. (D) The non-tagged poNOD1 in HEK293 cells was stained by anti-poNOD1 antibody, followed by Alexa 488-conjugated anti-rabbit IgG (green). The inset shows the cells transiently transfected with control plasmid vector. The nuclei were stained with SYTOX orange (red). Representative sections from one of six independent experiments are shown. Scale bars = 10 μm. (For interpretation of the references to color in this figure legend, the reader is referred to the web version of the article.)

NF-κB was slightly but significantly activated following a 24-h stimulation with *meso*-DAP but not following stimulation with DD- or LL-DAP. We found that *meso*-lanthionine also activates HEK293^{poNOD1} cells, resulting in a significant enhancement of NF-κB activity. The activation of NF-κB by stimulation with *meso*-DAP or *meso*-lanthionine was augmented by the simultaneous treatment with cytochalasin D (Fig. 4B). Furthermore, the three isomers of DAP and *meso*-lanthionine were completely inactive in HEK293^{Cont} cells (data not shown). Although the activities of *meso*-DAP and *meso*-lanthionine were smaller than the known minimum NOD1 agonist iE-DAP, they did show specific activity as NOD1 ligands (Figs. 3 and 4).

3.5. Expression of NOD1 in newborn and adult swine tissues

We used real-time quantitative PCR to analyze the expression of NOD1 mRNA in newborn and adult swine tissues. As shown in Fig. 5, NOD1 mRNA was expressed at detectable levels in all newborn and adult swine tissues examined. In the newborn swine immediately after birth, NOD1 mRNA was most strongly expressed in the MLNs. The expression levels in other tissues decreased in the following order: esophagus > spleen > ileal Pps > ileum > colon > duodenum > jejunum (Fig. 5A). Relatively lower expression levels of NOD1 were found in digestive tissues except for the esophagus.

In the adult swine, similar expression patterns were observed, with the highest levels found in GALTs (MLNs and ileal Pps) and esophagus (Fig. 5B). However, in contrast to newborns, when the expression levels of NOD1 were calculated relative to spleen, they were higher in adult MLNs and all digestive tissues (Fig. 5A and B). These results suggest that NOD1 plays an important role in the induction of immune responses, especially in the esophagus and GALTs of adult and newborn swine.

3.6. Up-regulation of NOD1 expression after stimulation with PAMPs and lactic acid bacteria in adult and newborn swine GALT

The GALT is an important front line of host defense and is confronted with a large amount of immunomodulating PAMPs.

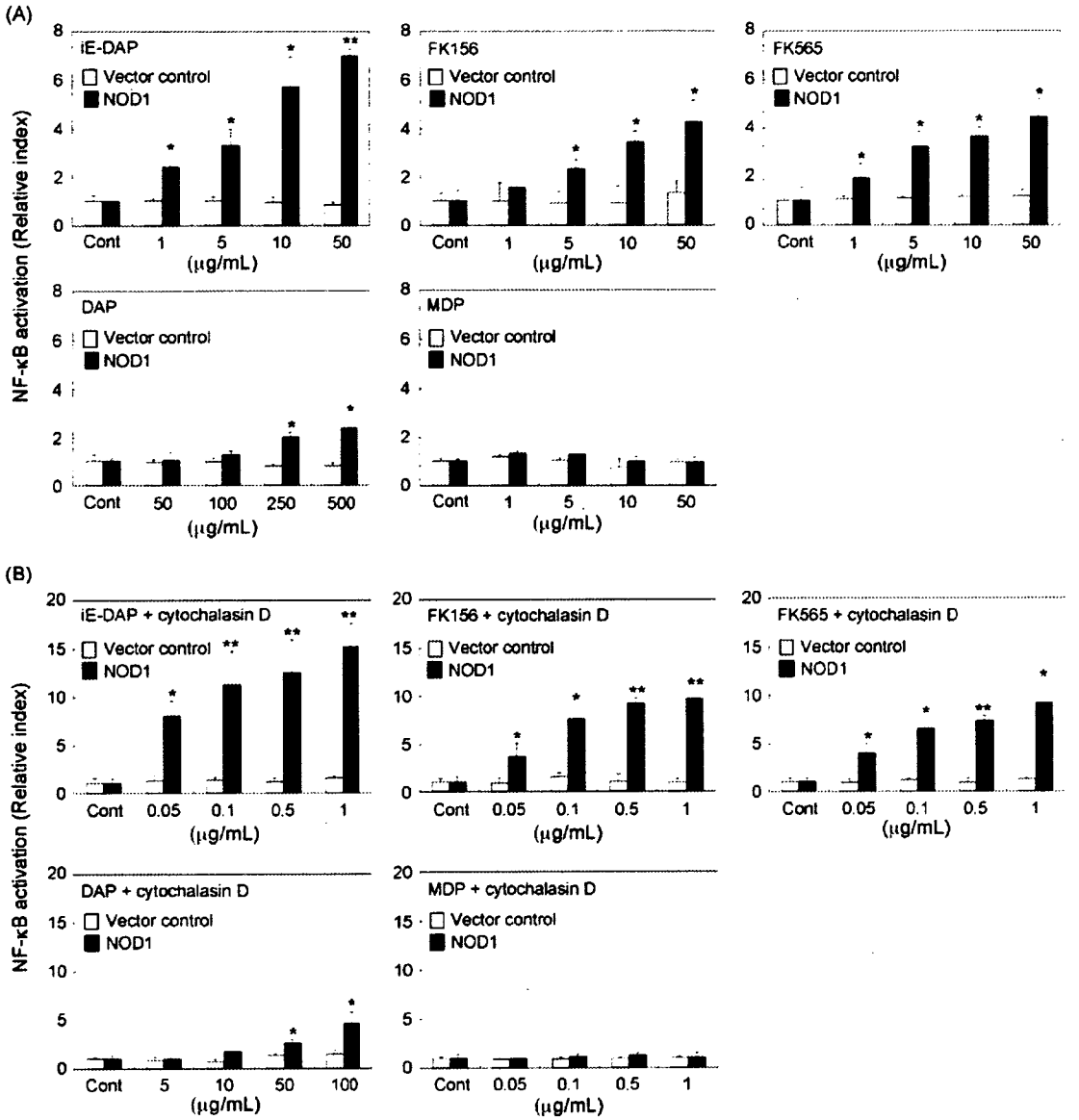

Fig. 3. Induction of NF-κB reporter (luciferase) activity by various chemically synthesized low-molecular weight PGN fragments via poNOD1. HEK293^{Cont} or HEK293^{poNOD1} cells were treated with the indicated concentrations of PGN fragments for 24 h without (A) or with (B) pretreatment with cytochalasin D (CytoD; 1 μM) for 30 min. Values represent means, and error bars indicate the S.D. The results are representative of three or four independent experiments. *$P < 0.05$; **$P < 0.01$ vs. cells treated without stimulants.

To assess the induction of NOD1 expression in GALT via TLRs and the NOD signaling pathway, we analyzed the effects of various PAMPs on the expression of NOD1 in adult and newborn swine GALT, namely, the MLNs and Pps. In the current study, we used the synthetic bacterial lipopeptide Pam3Cys as an agonist for TLR2, synthetic CpG DNA motif CpG2006-TGTT as an agonist for TLR9, MDP as an agonist for NOD2, and iE-DAP as a strongest agonist for NOD1. In addition to these synthetic agonists, we tested two strains of immunobiotic lactic acid bacteria. For the individual ligands, titration studies were performed to determine the optimal concentrations for the experimental systems (data not shown).

In the adult swine MLNs and Pps, MDP, Pam3Cys, CpG2006-TGTT and the two strains of lactic acid bacteria strongly induced the expression levels of NOD1 gene transcripts in a the time-dependent manner (Fig. 6). In the immature ileal Pps and MLNs, these ligands tend to enhance the expression of NOD1, and significant up-regulation was observed after a 6-h stimulation (Fig. 6). In addition, iE-DAP itself also caused a striking increase in the expression of NOD1 in adult and newborn GALT (Fig. 6), indicating that NOD1 signaling cascades lead to the induction of its expression. The two other NOD1 ligands, FK156 and FK565, significantly enhanced the expression of NOD1 to a similar extent as iE-DAP, whereas *meso*-DAP and *meso*-lanthionine had relatively little activity, and LL- and DD-DAP were inactive (data not shown). Furthermore, the level of NOD1 induction by TLR and NOD agonists was higher in the GALT of adults than of newborns.

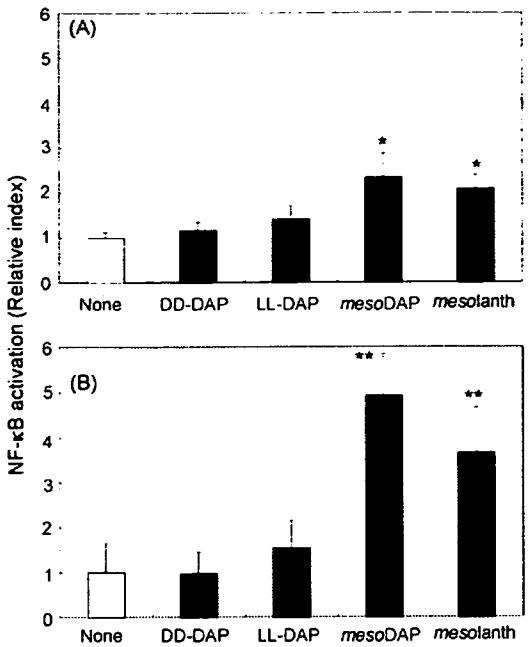

Fig. 4. Activation of NF-κB in HEK293^{poNOD1} cells by *meso*-DAP and *meso*-lantionine. HEK293^{poNOD1} cells were treated with LL-DAP (250 μg/mL), DD-DAP (250 μg/mL), *meso*-DAP (250 μg/mL), or *meso*-lantionine (*meso*-lanti; 250 μg/mL) for 24 h without (A) or with (B) pretreatment with cytochalasin D (1 μM) for 30 min. Values represent means, and error bars indicate the standard deviations. The results are representative of three or four independent experiments. $*P<0.05$; $**P<0.01$ vs. cells treated without stimulants.

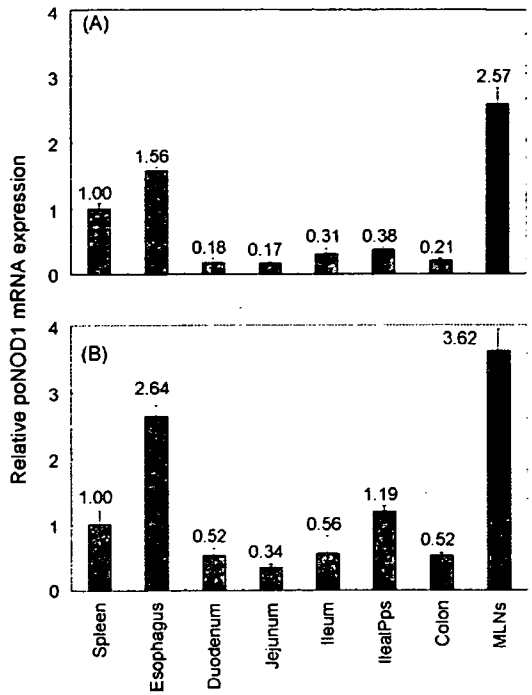

Fig. 5. Analysis of NOD1 expression in newborn (A) and adult (B) swine tissues by real-time quantitative PCR. The level of poNOD1 mRNA was normalized by the level of porcine β-actin mRNA, and the relative index was determined relative to the NOD1 mRNA level in spleen (1.00). Values represent means, and error bars indicate the standard deviations. The results are representative of three independent experiments using tissues from at least three individual newborn or adult swine.

4. Discussion

In the current study, we cloned poNOD1 cDNA and characterized the functional domains in the protein sequence. The open reading frame of poNOD1 was 2862 bp, corresponding to a 953-amino acid polypeptide. Characterization of poNOD1 showed that it is an intracellular receptor that possesses the typical structure of human and mouse NOD1. Similarities in amino acid sequence and a phylogenetic tree based revealed that nucleotide

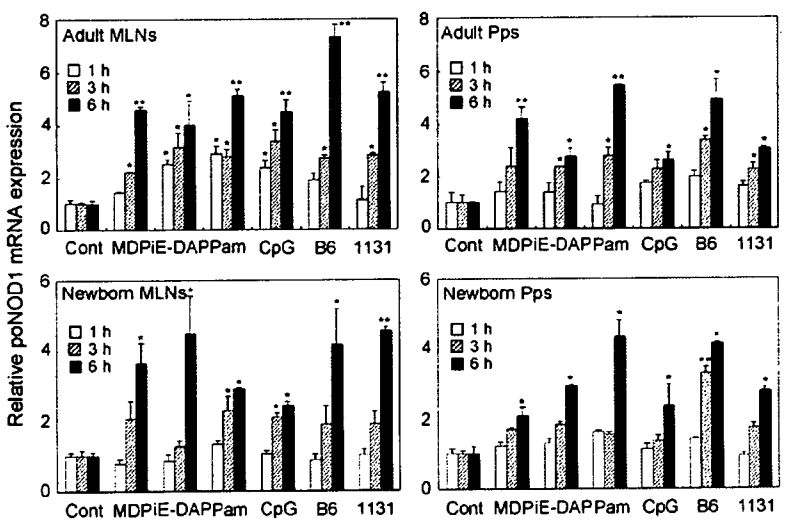

Fig. 6. Induction of NOD1 in MLNs and ileal Pps of adult and newborn swine. Cells (2×10^6 cells) from MLNs and ileal Pps were cultured in the absence (Cont) or presence of muramyl dipeptide (MDP; 50 μg/mL), iE-DAP (50 μg/mL), Pam3Cys (Pam; 1 ng/mL), CpG2006-TGTT (CpG; 1 μM), *L. gasseri* JCM1131^T (1131; 100 μg/mL), or *L. bulgaricus* NIA1 B6 (B6; 100 μg/mL) for the indicated times. The expression of poNOD1 mRNA was determined by real-time PCR. Results are expressed as the relative mRNA index, calculated as the mRNA index (estimated poNOD1 mRNA copy number/estimated porcine β-actin mRNA copy number) of stimulated cells divided by the mRNA index of unstimulated cells. Columns represent the mean relative index, and error bars indicate the S.E. Each experiment was repeated three times. $**P<0.01$ and $*P<0.05$ vs. cells cultured in the absence of stimulants.

and amino acid sequences of poNOD1 were more closely related to NOD1 of human than mouse, supporting the idea that swine are a better model for the human immune system than mice (Shimosato et al., 2005a; Tohno et al., 2005a).

Another NOD receptor, NOD2, has been reported to associate with the plasma membrane in human and swine (Lécine et al., 2007; Tohno et al., 2008), but the precise subcellular pattern of NOD1 expression has not been well characterized. In the present study, overexpression of poNOD1 in HEK293 cells revealed that it is located not only in the cytoplasm but also on the inner side of the plasma membrane. Recently, membrane association of human NOD2 was reported to be required for the membrane recruitment of Rip-like interacting caspase-like apoptosis-regulatory protein kinase, which induces NF-κB signaling and the production of proinflammatory cytokines (Lécine et al., 2007). Our current results demonstrated for the first time that, like NOD2, NOD1 can bind to the plasma membrane, suggesting that membrane-bound NOD1 mediates activation of the NF-κB pathway from the plasma membrane. Additional studies are needed to resolve the immunologic significance of membrane-bound NOD1.

The optimal peptidoglycan motifs recognized by human and mouse NOD have been reported to be quite different (Takada and Kotani, 1995; Magalhaes et al., 2005; Takada and Uehara, 2006). In mice, the NOD2 agonist MDP alone does not induce the production of cytokines, although it causes a strong cytokine induction in other animals (Takada and Kotani, 1995). Interestingly, for NOD1 ligands, the optimal unit for activating human cells (L-Ala-γ-D-Glu-*meso*-DAP) appears different from that for mouse cells (L-Ala-D-glu-*meso*-DAP-D-Ala) (Girardin et al., 2003c; Magalhaes et al., 2005). Therefore, it appears that the use of other animal models such as swine is important for understanding immunomodulation via human NOD both *in vitro* and *in vivo*. For this reason, poNOD1 recognition of PGN fragments needs to be fully characterized. When NOD1 was first identified, Girardin et al. (2003c) and Chamaillard et al. (2003) reported that the dipeptide iE-DAP is the minimum PGN structure capable of activating human NOD1. More recent studies by Uehara et al. (2006) defined the structures sufficient for immunoactivation via human NOD1 as *meso*-DAP and *meso*-lanthionine. Further studies in a variety of species are need to resolve the discrepancy between these results.

In the present study, we found that *meso*-DAP activates NF-κB in HEK293^{poNOD1} cells. In addition, LL-DAP, which has been isolated from certain bacteria including *Clostridium perfringens*, *Propionibacterium acnes* and *Porphyromonas gingivalis* weakly activated NF-κB in permeabilized HEK293^{poNOD1} cells (relative index = 1.53 in Fig. 5B), whereas DD-DAP, which has not yet been found in any bacteria, was completely inactive. Furthermore, we showed that poNOD1 also recognizes a synthetic *meso*-lanthionine that is a counterpart to *meso*-DAP in some *Fusobacteria* and related species such as *Fusobacterium nucleatum* (Kato et al., 1979, 1981; Vasstrand et al., 1979). As found in NOD1-positive human epithelial cells and monocytes (Uehara et al., 2006), the most potent activator of NF-κB in HEK293^{poNOD1} cells was iE-DAP, followed by DMPs such as FK156 and FK565, and slight but significant activation by *meso*-DAP and *meso*-lanthionine. These findings suggest that ligand specificity is similar between porcine and human NOD1. These findings also suggest that *meso*-DAP and *meso*-lanthionine are the minimal agonists for inducing immunoactivation via NOD1.

MDP and DMPs are strong cytokine inducers in human blood monocytes, although much higher levels of low-molecular weight PGN fragments including *meso*-DAP (up to several hundred micrograms per milliliter) than TLR ligands are required to induce comparable immunoactivation (Takada and Uehara, 2006; Uehara et al., 2006). Because NOD proteins are intracellular receptors, higher concentrations of their ligands are needed for immunoactivation (Takada and Uehara, 2006; Uehara et al., 2006). Therefore, as described previously (Magalhaes et al., 2005), we used cytochalasin D to enhance the stimulation by NOD ligands. Indeed, we found that cytochalasin D enhanced the activation of NF-κB in HEK293^{poNOD1} by NOD1 ligands. Specifically, 250 μg/mL of *meso*-DAP or *meso*-lanthionine maximally activated NF-κB in the presence of cytochalasin D (Fig. 4B). Stimulation by these two ligands with cytochalasin D was also observed at ligand concentrations of 0.5 μg/mL (data not shown). Although that apical peptide transporter PEPT1 may deliver MDP and subsequently activate NF-κB via NOD2 (Ismair et al., 2006), how the NOD1-activating PGN fragments enter the cytoplasm is currently unknown. Regardless, our results indicate that the cloned poNOD1 is functionally expressed in the intracellular compartment and that it is activated not only by iE-DAP but also *meso*-DAP and *meso*-lanthionine when they are delivered into the cytoplasm.

Although NOD1 is expressed in many tissues including epithelial cells and antigen-presenting cells (Strober et al., 2006), the relative expression in the digestive tissues has not been fully examined. In the current study, high levels of poNOD1 were observed especially in the esophagus and GALT, such as the ileal Pps and MLNs, of newborn and adult swine. In newborn swine, expression of NOD1 was lower than in the adult in intestinal tissues that are directly exposed to intestinal bacteria during adulthood. It has been reported that the expression of NOD1 in intestinal epithelial cells is up-regulated by pro-inflammatory cytokines produced in response to bacterial products (Hisamatsu et al., 2003). Therefore, our results suggest that the lower levels of NOD1 expression in immature intestinal tissues of newborn swine are due to a lower exposure to intestinal bacterial flora. Additionally, the finding of different expression levels of NOD1 in newborn and adult digestive tissues and MLNs suggests that the intestinal microflora directly promote the expression of NOD1 in these tissues during postnatal development.

In the Pps and MLNs of adult and newborns, chemically synthesized PAMPs including Pam3Cys, CpG2006-TGTT, MDP, and iE-DAP strongly enhanced the expression of NOD1. The degree of NOD1 induction by TLR and NOD ligands was higher in GALT of adults than of newborns. Our current results and those of by Tohno et al. (2006, 2008) indicate that this is due to the higher expression of TLR2, TLR9, NOD1, and NOD2 in the GALT of adults than newborn swine. These results indicate that the activation of signaling pathways downstream of TLR2, TLR9, NOD1, and NOD2 leads

to the up-regulation of NOD1 expression. In intestinal epithelial cells, pro-inflammatory cytokines such as interferon (IFN)-γ are involved in the induction of NOD1 transcription (Hisamatsu et al., 2003). Promoter analysis for NOD1 indicates that the interferon regulatory factor-1 binding motif is essential for the effect of IFN-γ (Hisamatsu et al., 2003). In our previous study, we showed that GALT of newborn and adult swine produce IFN-γ in response to TLR2 and TLR9 activation (Tohno et al., 2006; Shimosato et al., 2006). Therefore, our current findings support the idea that ligands of TLRs and NODs enhance NOD1 expression in part by inducing the production of IFN-γ.

In addition, we found that two strains of lactic acid bacteria, *L. gasseri* JCM1131^T and *L. bulgaricus* NIAI B6, which cell wall contains lysine-type PGN, potently enhance NOD1 expression in adult and newborn GALT. We previously demonstrated that these two strains and their bacterial components are recognized by porcine TLR2 and TLR9 (Tohno et al., 2005b; Shimosato et al., 2006). These current findings suggest that immunobiotic lactic acid bacteria directly promote the transcription of NOD1 via TLR and NOD during postnatal development of the GALT, resulting in a high level of NOD1 expression in the adult GALT. Thus, oral vaccines and functional foods containing immunobiotic lactic acid bacteria may promote the development of NOD1 recognition in the GALT.

In conclusion, we found that poNOD1 is more closely related to the human protein than the mouse counterpart and that it is expressed not only in the cytoplasm but also on the inner side of the plasma membrane. We also found that the binding of poNOD1 by *meso*-DAP and *meso*-lanthionine leads to NF-κB activation. Thus, NOD1, which is strongly expressed in the GALT, may be an important immunoregulator of intestinal immunity in swine. Clarification of the role of poNOD1 in the regulation of the swine GALT is important for it development as a model for of the human mucosal immune system.

Acknowledgements

We sincerely thank Dr. T. Shimosato (Laboratory of Experimental Immunology, Center for Cancer Research, National Cancer Institute at Frederick, USA), Drs. Y. Kawai, S. Katoh and Y. Azuma (Laboratory of Animal Products Chemistry, Graduate School of Agricultural Science, Tohoku University) for helpful technical supports and discussions, and Dr. H. Inadera (Department of Public Health, Toyama Medical and Pharmaceutical University, Japan) for the gift of the pGLM-ENH-luci vector. This study was partly supported by a Grant-in-Aid for Scientific Research (B) (2) (No. 18380158) from the Japan Society for the Promotion of Science, an NISR Research Grant from the Noda Institute for Scientific Research to Dr. H. Kitazawa, and a grant from the Secure and Healthy Animal Production project from the Ministry of Agriculture, Forestry and Fisheries of Japan to Dr. H. Aso and Dr. H. Kitazawa. M. Tohno is a supported JSPS research fellow (Research Fellowships for Young Scientists Program, No. 18005121).

Appendix A. Supplementary data

Supplementary data associated with this article can be found, in the online version, at doi:10.1016/j.molimm.2007.09.029.

References

Adam, A., 1985. Muramylpeptides and Analogues Synthetic Adjuvants. Wiley, Chichester, UK, pp. 1–58.

Chamaillard, M., Hashimoto, M., Horie, Y., Masumoto, J., Qiu, S., Saab, L., Ogura, Y., Kawasaki, A., Fukase, K., Kusumoto, S., Valvano, M.A., Foster, S.J., Mak, T.W., Nuñez, G., Inohara, N., 2003. An essential role for NOD1 in host recognition of bacterial peptidoglycan containing diaminopimelic acid. Nat. Immunol. 4, 702–707.

Ellouz, F., Adam, A., Ciorbaru, R., Lederer, E., 1974. Minimal structural requirements for adjuvant activity of bacterial peptidoglycan derivatives. Biochem. Biophys. Res. Com. 59, 1317–1325.

Girardin, S.E., Boneca, I.G., Viala, J., Chamaillard, M., Labigne, A., Thomas, G., Philpott, D.J., Sansonetti, P.J., 2003a. Nod2 is a general sensor of peptidoglycan through muramyl dipeptide (MDP) detection. J. Biol. Chem. 278, 8869–8872.

Girardin, S.E., Boneca, I.G., Carneiro, L.A., Antignac, A., Jéhanno, M., Viala, J., Tedin, K., Taha, M.K., Labigne, A., Zähringer, U., Coyle, A.J., DiStefano, P.S., Bertin, J., Sansonetti, P.J., Philpott, D.J., 2003b. Nod1 detects a unique muropeptide from gram-negative bacterial peptidoglycan. Science 300, 1584–1587.

Girardin, S.E., Travassos, L.H., Hervé, M., Blanot, D., Boneca, I.G., Philpott, D.J., Sansonetti, P.J., Mengin-Lecreulx, D., 2003c. Peptidoglycan molecular requirements allowing detection by Nod1 and Nod2. J. Biol. Chem. 278, 41702–41708.

Goto, T., Aoki, H., 1987. The immunomodulatory activities of acylpeptides. In: Azuma, I., Jollès, G. (Eds.), Immunostimulants: Now and Tomorrow. Springer-Verlag, Berlin, pp. 99–108.

Hisamatsu, T., Suzuki, M., Podolsky, D.K., 2003. Interferon-gamma augments CARD4/NOD1 gene and protein expression through interferon regulatory factor-1 in intestinal epithelial cells. J. Biol. Chem. 278, 32962–32968.

Inohara, N., Nuñez, G., 2003. NODs: intracellular proteins involved in inflammation and apoptosis. Nat. Rev. Immunol. 3, 371–382.

Inohara, N., Ogura, Y., Fontalba, A., Gutierrez, O., Pons, F., Crespo, J., Fukase, K., Inamura, S., Kusumoto, S., Hashimoto, M., Foster, S.J., Moran, A.P., Fernandez-Luna, J.L., Nuñez, G., 2003. Host recognition of bacterial muramyl dipeptide mediated through NOD2 Implications for Crohn's disease. J. Biol. Chem. 278, 5509–5512.

Ismair, M.G., Vavricka, S.R., Kullak-Ublick, G.A., Fried, M., Mengin-Lecreulx, D., Girardin, S.E., 2006. hPepT1 selectively transports muramyl dipeptide but not Nod1-activating muramyl peptides. Can. J. Physiol. Pharmacol. 84, 1313–1319.

Kato, K., Umemoto, T., Sagawa, H., Kotani, S., 1979. Lanthionine as an essential constituent of cell wall peptidoglycan of *Fusobacterium nucleatum*. Curr. Microbiol. 3, 147–151.

Kato, K., Umemoto, T., Fukuhara, H., Sagawa, H., Kotani, S., 1981. Variation of dibasic amino acid in the cell wall peptidoglycan of bacteria of genus *Fusobacterium*. FEMS Microbiol. Lett. 10, 81–85.

Kitaura, Y., Nakaguchi, O., Takeno, H., Okada, S., Yonishi, S., Hemmi, K., Mori, J., Senoh, H., Mine, Y., Hashimoto, M., 1982. N2-(Gamma-D-glutamyl)-*meso*-2(L) 2′(D)-diaminopimelic acid as the minimal prerequisite structure of FK-156: its acyl derivatives with potent immunostimulating activity. J. Med. Chem. 25, 335–337.

Kotani, S., Watanabe, Y., Kinoshita, F., Shimono, T., Morisaki, I., 1975. Immunoadjuvant activities of synthetic *N*-acetylmuramyl-peptides or -amino acids. Biken J. 18, 105–111.

Lécine, P., Esmiol, S., Métais, J.Y., Nicoletti, C., Nourry, C., McDonald, C., Nuñez, G., Hugot, J.P., Borg, J.P., Ollendorff, V., 2007. The NOD2-RICK complex signals from the plasma membrane. J. Biol. Chem. 282, 15197–15207.

Magalhaes, J.G., Philpott, D.J., Nahori, M.A., Jehanno, M., Fritz, J., Bourhis, L.L., Viala, J., Hugot, J.P., Giovannini, M., Bertin, J., Lepoivre, M., Mengin-Lecreulx, D., Sansonetti, P.J., Girardin, S.E., 2005. Murine Nod1 but not its human orthologue mediates innate immune detection of tracheal cytotoxin. EMBO Rep. 6, 1201–1207.

Meylan, E., Tschopp, J., Karin, M., 2006. Intracellular pattern recognition receptors in the host response. Nature 442, 39–44.

Myhre, A.E., Aasen, A.O., Thiemermann, C., Wang, J.E., 2006. Peptidoglycan—an endotoxin in its own right? Shock 25, 227–235.

Photaki, I., Samouilidis, I., Caranikas, S., Zervas, L., 1979. Lanthionine chemistry. Part 4. Synthyesis of diasteroisomeric cyclolanthionyl derivatives. J. Chem. Soc. Perkin Trans. 1, 2599–2605.

Shimosato, T., Kitazawa, H., Katoh, S., Tomioka, Y., Karima, R., Ueha, S., Kawai, Y., Hishinuma, T., Matsushima, K., Saito, T., 2003. Swine Toll-like receptor 9 recognizes CpG motifs of human cell stimulant. Biochim. Biophys. Acta 1627, 56–61.

Shimosato, T., Kitazawa, H., Tohno, M., Katoh, S., Kawai, Y., Saito, T., 2004. Development of immune assay system for both CpG and non-CpG DNA from lactic acid bacteria using a transfectant of swine Toll-like receptor 9. Anim. Sci. J. 75, 377–382.

Shimosato, T., Tohno, M., Kitazawa, H., Katoh, S., Watanabe, K., Kawai, Y., Aso, H., Yamaguchi, T., Saito, T., 2005a. Toll-like receptor 9 is expressed on follicle-associated epithelia containing M cells in swine Peyer's patches. Immunol. Lett. 98, 83–89.

Shimosato, T., Kitazawa, H., Katoh, S., Tohno, M., Iliev, I.D., Nagasawa, C., Kimura, T., Kawai, Y., Saito, T., 2005b. Augmentation of T(H)-1 type response by immunoactive AT oligonucleotide from lactic acid bacteria via Toll-like receptor 9 signaling. Biochem. Biophys. Res. Commun. 326, 782–787.

Shimosato, T., Kimura, T., Tohno, M., Iliev, I.D., Katoh, S., Ito, Y., Kawai, Y., Sasaki, T., Saito, T., Kitazawa, H., 2006. Strong immunostimulatory activity of AT- oligodeoxynucleotide requires a six-base loop with a self-stabilized 5′-C. G-3′ stem structure. Cell. Microbiol. 8, 485–495.

Strober, W., Murray, P.J., Kitani, A., Watanabe, T., 2006. Signalling pathways and molecular interactions of NOD1 and NOD2. Nat. Rev. Immunol. 6, 9–20.

Takada, H., Kotani, S., 1985. Immunopharmacological activities of synthetic muramyl-peptides. In: Stewart-Tull, D.E.S., Davies, M. (Eds.), Immunology of the Bacterial Cell Envelope. John Wiley & Sons, Chichester, UK, pp. 119–152.

Takada, H., Kotani, S., 1995. Muramyl dipeptide and derivatives. In: Stewart-Tull, D.E.S., Davies, M. (Eds.), The Theory and Practical Application of Adjuvants. John Wiley & Sons, Chichester, UK, pp. 171–202.

Takada, H., Uehara, A., 2006. Enhancement of TLR-mediated innate immune responses by peptidoglycans through NOD signaling. Curr. Pharm. Des. 12, 4163–4172.

Tohno, M., Shimosato, T., Kitazawa, H., Katoh, S., Iliev, I.D., Kimura, T., Kawai, Y., Watanabe, K., Aso, H., Yamaguchi, T., Saito, T., 2005a. Toll-like receptor 2 is expressed on the intestinal M cells in swine. Biochem. Biophys. Res. Commun. 330, 547–554.

Tohno, M., Kitazawa, H., Shimosato, T., Matsumoto, M., Katoh, S., Kawai, Y., Saito, T., 2005b. A swine toll-like receptor 2-expressing transfectant as a potential primary screening system for immunobiotic microorganisms. FEMS Immunol. Med. Microbiol. 44, 283–288.

Tohno, M., Shimosato, T., Moue, M., Aso, H., Watanabe, K., Kawai, Y., Yamaguchi, T., Saito, T., Kitazawa, H., 2006. Toll-like receptor 2 and 9 are expressed and functional in gut-associated lymphoid tissues of presuckling newborn swine. Vet. Res. 37, 1–22.

Tohno, M., Shimazu, T., Ueda, W., Anzawa, D., Aso, H., Nishimura, J., Kawai, Y., Saito, Y., Saito, T., Kitazawa, H., 2007a. Molecular cloning of porcine RP105/MD-1 involved in recognition of extracellular phosphopolysaccharides from *Lactococcus lactis* ssp. *cremoris*. Mol. Immunol. 44, 2566–2577.

Tohno, M., Shimosato, T., Kawai, Y., Aso, H., Ikegami, H., Taketomo, N., Saito, T., Kitazawa, H., 2007b. Advanced molecular immunoassay system for immunobiotic lactic acid bacteria using a transfectant of Toll-like receptor 2. Anim. Sci. J. 78, 195–205.

Tohno, M., Ueda, W., Azuma, Y., Shimazu, T., Katoh, S., Wang, J.M., Aso, H., Takada, H., Kawai, Y., Saito, T., Kitazawa, H., 2008. Molecular cloning and functional characterization of porcine nucleotide-binding oligomerization domain-2 (NOD2). Mol. Immunol. 45, 194–203.

Uehara, A., Fujimoto, Y., Kawasaki, A., Kusumoto, S., Fukase, K., Takada, H., 2006. *meso*-Diaminopimelic acid and *meso*-lanthionine, amino acids specific to bacterial peptidoglycans, activate human epithelial cells through NOD1. J. Immunol. 177, 1796–1804.

Vasstrand, E.N., Hofstad, T., Endresen, C., Jensen, H.B., 1979. Demonstration of lanthionine as a natural constituent of the peptidoglycan of *Fusobacterium nucleatum*. Infect. Immun. 25, 775–780.

Viala, J., Chaput, C., Boneca, I.G., Cardona, A., Girardin, S.E., Moran, A.P., Athman, R., Memet, S., Huerre, M.R., Coyle, A.J., DiStefano, P.S., Sansonetti, P.J., Labigne, A., Bertin, J., Philpott, D.J., Ferrero, R.L., 2004. Nod1 responds to peptidoglycan delivered by the Helicobacter pylori cag pathogenicity island. Nat. Immunol. 5, 1166–1174.

«paper no. jmm47679 charlesworth ref: jmm47679»

Oral microbiology

Journal of Medical Microbiology (2008), 57, 000–000 DOI 10.1099/jmm.0.47679-0

Dual regulation of interleukin-8 production in human oral epithelial cells upon stimulation with gingipains from *Porphyromonas gingivalis*

Akiko Uehara,[1] Mariko Naito,[2] Takahisa Imamura,[3] Jan Potempa,[4,5] James Travis,[5] Koji Nakayama[2] and Haruhiko Takada[1]

Correspondence
Akiko Uehara
kyoro@mail.tains.tohoku.ac.jp

[1]Department of Microbiology and Immunology, Tohoku University Graduate School of Dentistry, Sendai, Japan

[2]Division of Microbiology and Oral Infection, Department of Molecular Microbiology and Immunology, Nagasaki University Graduate School of Biomedical Sciences, Nagasaki, Japan

[3]Division of Molecular Pathology, Graduate School of Medical and Pharmaceutical Sciences, Kumamoto University, Kumamoto, Japan

[4]Department of Microbiology, Faculty of Biotechnology, Jagiellonian University, Kraków, Poland

[5]Department of Biochemistry and Molecular Biology, University of Georgia, Athens, GA, USA

Cysteine proteinases from *Porphyromonas gingivalis*, or gingipains, are considered to be key virulence factors of the bacterium in relation to periodontal diseases. Incubation of human oral epithelial cells with lysine-specific gingipain (Kgp) and high-molecular-mass arginine-specific gingipain (HRgpA) resulted in a decrease in the production of interleukin (IL)-8, but not in the production of other pro-inflammatory cytokines. In contrast, arginine-specific gingipain 2 (RgpB) increased IL-8 production. RNA interference assays demonstrated that Kgp- and HRgpA-mediated downregulation and RgpB-mediated upregulation occurred through protease-activated receptor (PAR)-1 and PAR-2 signalling. Although the RgpB-mediated upregulation of IL-8 production occurred through nuclear factor-kappa B (NF-κB), the Kgp- and HRgpA-mediated downregulation was not negated in NF-κB-silenced cells. Both the haemagglutinin and the enzymic domains are required for Kgp and HRgpA to downregulate the production of IL-8 in human oral epithelial cells, and the two domains are thought to co-exist. These results suggest that gingipains preferentially suppress IL-8, resulting in attenuation of the cellular recognition of bacteria, and as a consequence, sustain chronic inflammation.

Received 8 October 2007
Accepted 19 December 2007

INTRODUCTION

Periodontitis is an inflammation of the whole periodontium. The dominant cells in periodontal epithelial tissue are the oral epithelial cells. The barrier function of oral epithelial cells is mainly due to the production of antimicrobial peptides, such as human β-defensins and cathelicidin (Acheson & Luccioli, 2004). Healthy gingival epithelium is characterized by the presence of human β-defensin-2 and a gradient of interleukin (IL)-8 that guides the transmigration of leukocytes (Dixon *et al.*, 2004; Pütsep *et al.*, 2002). Inflamed gingival epithelium is severely infiltrated with leukocytes around the periodontal pocket (gingival crevice), accompanied by elevated expression of IL-8 (Liu *et al.*, 2001). Chemokines such as IL-8 form the first line of host defence by increasing phagocytosis, bacterial killing, the release of lysosomal enzymes and superoxide anion generation (Weiss, 1989), indicating that this mechanism is of great importance for innate immunity. *Porphyromonas gingivalis* has been implicated not only in severe chronic periodontitis, but also in aggressive periodontitis (Holt & Bramanti, 1991). *P. gingivalis* possesses a number of putative virulence factors, such as LPS, fimbriae and proteinases (Chen *et al.*, 1992). We have studied the virulence activities of two types of trypsin-like cysteine proteinase (Potempa *et al.*, 1995) that cleave specifically at Arg–X (50 and 95 kDa) (Wingrove *et al.*, 1992) and Lys–X (105 kDa) bonds and are referred to as arginine-specific gingipain (Rgp) and lysine-specific gingipain (Kgp), respectively (Pike *et al.*, 1994). The

Abbreviations: FPR-cmk, Phe-Pro-Arg-chloromethyl ketone; GAPDH, glyceraldehyde-3-phosphate dehydrogenase; HRgpA, high-molecular-mass arginine-specific gingipain; IFN-γ, gamma interferon; IL, interleukin; Kgp, lysine-specific gingipain; NF-κB, nuclear factor-kappa B; PAR, protease-activated receptor; Rgp, arginine-specific gingipain; PAR-1AP, PAR-1 agonist peptide; PAR-2AP, PAR-2 agonist peptide; PAR-3AP, PAR-3 agonist peptide; siRNA, short interfering RNA; z-FKck, benzyloxycarbonyl-Phe-Lys-chloromethyl; TNF-α, tumour necrosis factor alpha.

95 kDa high-molecular-mass arginine-specific gingipain (HRgpA) and Kgp are a complex of the catalytic domain and the haemagglutinin/adhesin domain, and differ from the 50 kDa Rgp (RgpB), which lacks the latter domain. We have shown that gingipains cleave CD14 on human monocytes (Sugawara *et al.*, 2000) and gingival fibroblasts (Tada *et al.*, 2002), and ICAM-1 on human oral epithelial cells (Tada *et al.*, 2003), inhibiting the LPS-elicited defensive response of these cells against this pathogen, and interaction between epithelial cells and leukocytes, respectively, which facilitates *P. gingivalis* in evading the innate immunity. Thus, gingipains are important virulence factors of *P. gingivalis*.

Members of the protease-activated receptor (PAR) family are G protein-coupled receptors (Coughlin, 2000; Déry *et al.*, 1998; O'Brien *et al.*, 2001). There are four members of this family. As PARs are expressed in a wide variety of cell types, it was recently suggested that they may play important roles in pathophysiological processes such as growth, development, inflammation, tissue repair and pain (Coughlin, 2000; Déry *et al.*, 1998; O'Brien *et al.*, 2001). In fact, we demonstrated that neutrophil serine proteinase 3 activates human oral epithelial cells and human gingival fibroblasts via the PAR-2 pathway (Uehara *et al.*, 2003, 2002b). It has been reported that RgpB cleaves and activates PAR-2 on human neutrophils (Lourbakos *et al.*, 1998), induces IL-6 secretion by activating PAR-1 and PAR-2 on human oral epithelial KB cells (Lourbakos *et al.*, 2001a), and causes platelet aggregation via PARs (Lourbakos *et al.*, 2001b). Furthermore, RgpB induces neuropeptide release from dental pulp cells via PAR-2 signalling (Tancharoen *et al.*, 2005). Recently, we revealed that Rgps (HRgpA and RgpB) stimulated the production of hepatocyte growth factor through PAR-1 and PAR-2 in human gingival fibroblasts (Uehara *et al.*, 2005), which may be associated with both inflammatory and reparative processes of periodontal disease. PARs are important molecules that mediate gingipain stimuli to cells. In this study, we analysed the effects of gingipains on the production of cytokines, particularly IL-8, by oral epithelial cells and investigated the possible involvement of PARs in gingipain effects.

METHODS

Reagents. Human natural gamma interferon (IFN-γ) was provided by Hayashibara Biochemical Laboratories. Human recombinant (r)IL-1α and recombinant tumour necrosis factor alpha (TNF-α) were supplied by Dainippon Pharmaceutical. Phe-Pro-Arg-chloromethyl ketone (FPR-cmk) and benzyloxycarbonyl-Phe-Lys-chloromethyl (z-FKck) were obtained from Bachem Bioscience. PAR-1 agonist peptide (PAR-1AP; SFLLRN), PAR-2 agonist peptide (PAR-2AP; SLIGKV) and PAR-3 agonist peptide (PAR-3AP; TFRGAP) were synthesized by Takara. All other reagents were obtained from Sigma-Aldrich, unless otherwise indicated.

Purification and activation of gingipains. Three forms of gingipain – 95 kDa HRgpA, 50 kDa RgpB and 105 kDa Kgp – were purified from *P. gingivalis* HG66 culture supernatant, as described previously (Pike *et al.*, 1994; Potempa *et al.*, 1998). The purity of each enzyme was checked by SDS-PAGE. In a 10% Tricine gel, RgpB migrated as a single band with a mobility equivalent to a molecular mass of 48 kDa and homogeneity greater than 95% as determined using laser densitometric scanning of the gel. HRgpA resolved into four major bands and one minor band on SDS-PAGE (Pike *et al.*, 1994). The identity of each protein band was confirmed by N-terminal sequence analysis as being derived from the HRgpA polyprotein. The amount of active enzyme in each purified gingipain was determined by active-site titration using FPR-cmk and z-FKck for the Rgps and Kgp, respectively (Potempa *et al.*, 1997). The concentration of fully activated gingipain with cysteine was calculated from the amount of inhibitor needed for complete inactivation of the proteinases. Therefore, the concentrations of gingipains indicated in this paper are represented as those of active gingipains. The gingipains were activated by diluting to 10 μM in 0.2 M HEPES (pH 8), 5 mM $CaCl_2$ and 10 mM cysteine, and incubating at 37 °C for 10 min. The activated gingipains were then diluted with medium or buffer. To block their enzymic activity, the activated gingipains were incubated with the specific inhibitors FPR-cmk and z-FKck for 10 min at room temperature prior to use.

Construction of a strain producing Kgp proteinase without the adhesin domains in a Rgp/Kgp/adhesin-null mutant. The 1.6 kb *Eco*RV–*Sma*I DNA fragment (*cepA* DNA block) of pCS22 (gift from Dr Christine Seers, Cooperative Research Centre for Oral Health Science, School of Dental Science, University of Melbourne, Australia) was inserted into the *Sma*I site of pKD703 (Shoji *et al.*, 2004) with and without the 6.7 kb *Xho*I–*Not*I DNA fragment (*kgp'–'rgpB* chimeric gene DNA, blunt-ended) of pKD855 (Sato *et al.*, 2005) to yield plasmids pKD856 (*fimA*::[*kgp'–'rgpB cepA*]) and pKD857 (*fimA*::*cepA*), respectively. *Sca*I-linearized pKD856 or pKD857 was introduced into the Rgp/Kgp/adhesin-null mutant KDP153 (Naito *et al.*, 2006), resulting in the transformants KDP154 and KDP160, respectively. KDP160 produces Kgp proteinase without the adhesin domains from the *kgp'–'rgpB* chimeric gene.

Collection of supernatants of wild-type *P. gingivalis* and mutant *P. gingivalis* strains and preparation of the adhesin domains rHgp44 and rHbR. *P. gingivalis* 33277 was grown anaerobically to stationary phase in enriched brain heart infusion broth with menadione and haemin without antibiotics. Mutant strains *P. gingivalis* KDP133 (*rgpA rgpB*), *P. gingivalis* KDP136 (*rgpA rgpB kgp*) (Shi *et al.*, 1999), *P. gingivalis* KDP137 (*rgpA kgp hagA*) (Shi *et al.*, 1999), *P. gingivalis* KDP153 (*rgpA rgpB kgp hagA*), KDP160 (*rgpA rgpB kgp hagA fimA*::[kgp'–'rgpB]) and KDP161 (*rgpA rgpB kgp hagA fimA*) (Table 1) were grown anaerobically to stationary phase in enriched brain heart infusion broth with menadione, haemin and erythromycin (10 μg ml^{-1}). After 2 days of culture, supernatants were obtained by centrifugation at 10 000 *g* for 20 min at 4 °C and

Table 1. Phenotype of protein fractions prepared from culture supernatants of wild-type and various mutant *P. gingivalis* strains

Strain	*rgpA*	*rgpB*	*kgp*	*hagA*
33277	+	+	+	+
KDP133	+	+	+	+
KDP137	–	+	–	–
KDP136	–	–	–	+
KDP153	–	–	–	–
KDP160	–	–	+	–
KDP161	–	–	–	–